

The Chemical Compositions of the Type II Cepheids – The BL Her and W Vir Variables

Thomas Maas

*The W.J. McDonald Observatory, The University of Texas; Austin, TX 78712-1083
thomas_maas@hotmail.com*

Sunetra Giridhar

*Indian Institute of Astrophysics; Bangalore, 560034 India
giridhar@iiap.res.in*

David L. Lambert

*The W.J. McDonald Observatory; University of Texas; Austin, TX 78712-1083
dll@astro.as.utexas.edu*

ABSTRACT

Abundance analyses from high-resolution optical spectra are presented for 19 Type II Cepheids in the Galactic field. The sample includes both short-period (BL Her) and long-period (W Vir) stars. This is the first extensive abundance analysis of these variables. The C, N, and O abundances with similar spreads for the BL Her and W Vir show evidence for an atmosphere contaminated with 3α -process and CN-cycling products. A notable anomaly of the BL Her stars is an overabundance of Na by a factor of about five relative to their presumed initial abundances. This overabundance is not seen in the W Vir stars. The abundance anomalies running from mild to extreme in W Vir stars but not seen in the BL Her stars are attributed to dust-gas separation that provides an atmosphere deficient in elements of high condensation temperature, notably Al, Ca, Sc, Ti, and *s*-process elements. Such anomalies have previously been seen among RV Tau stars which represent a long-period extension of the variability enjoyed by the Type II Cepheids. Comments are offered on how the contrasting abundance anomalies of BL Her and W Vir stars may be explained in terms of the stars' evolution from the blue horizontal branch.

Subject headings: stars:abundances – stars:AGB and post-AGB – stars: variables:other (RV Tauri)

1. Introduction

Wallerstein (2002) remarks that Type II Cepheids “include most intrinsic variables with periods between 1 and about 50 days, except for the classical Cepheids and the shortest semi-regular variables of type M.” These bounds on the periods place the Type II Cepheids in the instability strip between the RR Lyrae stars at the short period limit and the RV Tau variables at the long period limit. Type II Cepheids fall into two classes: BL Her stars with periods of 1 to 5 days and the W Vir stars with periods longer than about 10 days with an indistinct boundary at about 20-30 days separating these stars from the RV Tau stars. Kraft (1972) drew attention to the period gap (6 to 9 days) between the BL Her and W Vir stars in globular clusters.

This paper is devoted to abundance determinations of field Type II Cepheids. Compositions of these stars have received scant attention from spectroscopists despite hints of unusual compositions. Oddly, neither W Vir nor BL Her, the two prototypes, have been subjected to a modern analysis. Quantitative spectroscopy based on modern model atmospheres and CCD spectra seems to be limited to TX Del (Andrievsky et al. 2002)¹ ST Pup, a star with RV Tau-like abundance anomalies (Gonzalez & Wallerstein 1996), and the C-rich stars V553 Cen and RT TrA (Wallerstein & Gonzalez 1996; Wallerstein et al. 2000). Model atmosphere analyses based on image-tube photographic spectra were reported for BL Her (Caldwell & Butler 1978), κ Pav (Luck & Bond 1989) and AU Peg (Harris, Olszewski, & Wallerstein 1984). Curve of growth analyses and photographic spectra provided abundance estimates for TW Cap (Anderson & Kraft 1971), W Vir (Barker et al. 1971), and κ Pav (Rodgers & Bell 1963, 1968). This very mixed bag of abundance estimates is an inadequate basis from which to draw conclusions concerning the evolution of Type II Cepheids and other potential origins for abundance anomalies.

The principal prior indication of an anomalous composition for Type II Cepheids concerns the reported deficiency of the *s*-process elements (relative to the iron abundance) – see Rodgers & Bell (1963, 1968), Barker et al. (1971) and especially Luck & Bond (1989). Our interest was driven in part by this indication, but also by the lack of a thorough study of field Type II Cepheids, and finally by their close relationship to the RV Tau stars for which abundance anomalies exist. The principal anomaly for some RV Tau stars is one in which the atmosphere is deficient in those elements that first condense into grains as gas is cooled, i.e., there has been a separation or winnowing of dust from gas and accretion of gas by the star (Giridhar et al. 2005). An apparently rarer anomaly is one in which elements with a low first ionization potential are underabundant (Rao & Reddy 2005). Other RV

¹Andrievsky et al. identified TX Del as a first-overtone Type I Cepheid - see below.

Tau stars have a normal composition. There is ample evidence that the W Vir and RV Tau stars have much in common. For example, photometry of Type II Cepheids and RV Tau stars in the LMC shows clearly that the RV Tau stars and the Type II Cepheids define a common Period-Luminosity-Color relation (Alcock et al. 1998). Given this commonality, the question naturally arises – What abundance anomalies are shown by the BL Her and W Vir stars and are those anomalies similar to those shown by the RV Tau stars?

The observations and abundance analyses of 19 Type II Cepheids are described in Section 2. Results for the individual stars and remarks on their classification as Type II Cepheids are provided in Section 3. Discussion of the possible anomalous abundances and their relation to the prior evolution of the stars and to other processes is provided in Section 4. Brief remarks on the spectroscopic calibration of photometric measurements of metallicity are given in Section 5. Concluding remarks are offered in Section 6.

2. Observations and Analyses

The program stars were observed with the W.J. McDonald Observatory’s 2.7m Harlan J. Smith reflector and the CCD-equipped ‘2dcoudé’ spectrograph (Tull et al. 1995) in observing runs in 2004 and 2005. A spectral resolving power $R = \lambda/\Delta\lambda \simeq 60,000$ was used and a broad spectral range was covered in a single exposure.

Spectra were rejected if they showed line doubling, markedly asymmetric lines, or strong emission in the Balmer lines. It is presumed that the spectra not showing these characteristics represent the atmosphere at a time when standard theoretical models may be applicable. This presumption should be tested by analysis of a series of spectra taken over the pulsational cycle. This remains to be done but we have analysed three stars using spectra taken at different phases and obtained consistent results. The program stars and dates of observation are listed in Table 1.

The abundance analyses were performed as described in our earlier papers on the RV Tau variables. Atmospheric parameters are determined from the Fe I and Fe II lines by demanding excitation and ionization equilibrium, and that the iron abundance be independent of the equivalent width. The adopted parameters listed in Table 1 were determined using Kurucz model atmospheres and a normal helium abundance ($\text{He}/\text{H} = 0.1$). The full abundance analysis used a Kurucz atmosphere with the parameters in Table 1. Abundances are referred to the recommended solar photospheric abundances given by Asplund, Grevesse, & Sauval (2005). Table 1 shows the anticipated average difference in atmospheric parameters ($T_{\text{eff}}, \log g$) between the BL Her and W Vir stars: $(T_{\text{eff}}, \log g) = (5970, 1.4)$ and $(5380, 0.6)$ for the

BL Her and W Vir stars, respectively.

3. The Program Stars

Harris (1985) provided what is regarded as the reference catalog of Type II Cepheids. His principal criterion for distinguishing a Type II from a Classical (Type I) Cepheid was distance from the Galactic plane ($|Z|$). Our selection of stars was based on his catalog but includes some recent discoveries. Various photometric indices extracted from the light curves have been proposed as distinctive marks of a Type II or a Type I Cepheid but the distinction remains tricky, as many authors remark. In addition, longer period Type II Cepheids overlap in pulsational properties (i.e., period and luminosity) with the RV Tau variables. Therefore, not only must population type be examined but variable type too. In the following text, we comment on our selection of Type II Cepheids and remark on those with RV Tau proclivities.

In this paper, the distinction between a BL Her and a W Vir variable is maintained; the reasons for this will become obvious when the compositions are presented. Here, a BL Her variable is one with a pulsation period of four days and shorter, and a W Vir variable is a star with a period of 11 days or longer. Four stars in the sample are of intermediate period with two judged by composition to be BL Her stars and two W Vir stars.

The stars are discussed in order of increasing pulsation period.

BX Del: BX Del with an estimated $|Z|$ of 0.3 kpc was listed as a Type II Cepheid by Harris (1985). The metallicity $[\text{Fe}/\text{H}] = -0.2$ places BX Del at about the upper limit for thick disk stars (Reddy et al. 2006).

VY Pyx: This variable was identified as a Type II Cepheid by Sanwal & Sarma (1991). The composition shows similarities with that of BX Del.

BL Her: This Type II Cepheid is the prototype of the subclass of the shorter period variables.

SW Tau: The light curve of this bright BL Her star is that of a Type II Cepheid. The metallicity, $[\text{Fe}/\text{H}]$ of +0.2, places SW Tau as the most metal-rich star in our sample. SW Tau is C-rich with the C I lines strong by inspection (Figure 1). This figure shows a portion of the spectrum of SW Tau, IX Cas (a very C-poor star), CC Lyr (a star of normal C abundance but having an extreme Fe-deficiency), and BL Her. The four stars have similar atmospheric parameters and, therefore, to first order the variations in the strength of a given line from star-to-star reflect abundance differences between the stars.

AU Peg: AU Peg is a single-lined spectroscopic binary (Harris, Olszewski, & Wallerstein 1984) with an orbital period of 53.3 days. Harris et al. argue that the secondary is a more massive compact object. A feature of AU Peg is that it lies close to or just beyond the red edge of the instability strip (Harris et al 1984; Vinkó, Szabados, & Szatmáry 1993). Presently, AU Peg is close to filling its Roche lobe and mass transfer between the two stars almost certainly occurred at an earlier time. Dust, as indicated by an IR-excess (McAlary & Welch 1986), surrounds the binary. Outflow from the system is suggested by the appearance of P Cygni-like feature accompanying AU Peg’s $H\alpha$ profile (Vinkó et al. 1998).

DQ And: Harris (1985) listed this star as a Type II Cepheid on the basis of the estimated distance from the Galactic plane: $|Z| = 0.6$ kpc. Balog, Vinkó, & Kaszás (1997), put $|Z|$ at 2.3 kpc. The radial velocity of -231 km s $^{-1}$ (Harris & Wallerstein 1984) is certainly not that expected of a Pop. I star. However, the Baade-Wesselink radius puts DQ And on the period-radius (P-R) relation defined by Classical Cepheids (Balog et al. 1997). The star is here considered to be of Type II.

UY Eri: With a $[Fe/H]$ of -1.8 and a radial velocity of 171 km s $^{-1}$ (Harris & Wallerstein 1984), UY Eri is obviously a Type II Cepheid and member of the Galactic halo. Its composition is typical of a halo star with $[Fe/H]$ of -1.8 (McWilliam 1997).

TX Del: Harris (1985) includes the star in his table of Type II Cepheids. Harris & Welch (1989) found that the star is a single-lined spectroscopic binary with an orbital period of 133 days. Schmidt et al. (2005) show that the star has varied in mean brightness, a characteristic not associated with a Classical Cepheid. Andrievsky et al. (2002) consider TX Del to be a first-overtone Classical Cepheid.² Although this identification may ease an explanation for the star’s solar metallicity, it places this Pop. I object more than 1 kpc from the Galactic plane. The Baade-Wesselink radius (Balog et al. 1997) places TX Del, as it does DQ And, on the P-R relation for Classical Cepheids. An explanation as a runaway star seems unlikely given that TX Del is a binary. We consider TX Del to be a Type II Cepheid and recall, as did Harris & Welch, the association of Pop. II characteristics and near-solar metallicity held by metal-rich RR Lyrae stars.

IX Cas: A Type II star according to Harris (1985) who gave $|Z|$ as 0.7 kpc. This is the primary of a spectroscopic binary (Harris & Welch 1989). The Baade-Wesselink radius puts the star on the Type II P-R line. The pulsation period of 9.2 days is long for a BL Her star but the high Na abundance which distinguishes BL Her from W Vir stars places this star among the BL Her class. The outstanding mark of IX Cas’s spectrum is the weakness

²Our derived abundances are in quite good agreement with those by Andrievsky et al. (2002); the mean difference in absolute abundance from 12 elements in common is -0.15 dex.

of the C I lines. Figure 1 shows that the C I lines typically used in our analyses are weak or absent from the spectrum of IX Cas. Lines near 9050 Å which are normally too strong for use in the abundance analysis had to be used in the case of IX Cas. The low C abundance is reminiscent of values found for the weak G-band giants (Snedden et al. 1978).

AL Vir: AL Vir is a Type II Cepheid according to distance from the Galactic plane (Harris 1985), light curve (Schmidt et al. 2004a), He I 5876 Å emission (Schmidt et al. 2004b), and the Baade-Wesselink radius (Balog et al. 1997). AL Vir with a pulsation period of 10.3 days marks the transition from BL Her to W Vir stars in our listing of variable by increasing period. The composition (particularly the lack of a Na overabundance) suggests AL Vir is a W Vir star.

AP Her: Harris (1985) considered AP Her a Type II Cepheid on the basis of the estimated $|Z|$ of 0.4 kpc. At $[Fe/H] \simeq -0.8$, this may be considered a thick disk star. The literature on Type II Cepheids is peppered with remarks about the difficulties in distinguishing between Type I and II Cepheids. This is well illustrated by Schmidt et al. (2004a) who, in a discussion of stars with large period changes, put AP Her with stars that ‘are likely type II Cepheids’ but later place AP Her among the variables ‘for which the predominance of the evidence indicates type I classification’. The $[Fe/H]$ confirms that AP Her is not a Classical Cepheid.

CO Pup: The literature on this star is extremely sparse. Following Harris’s (1985) listing of CO Pup as a Type II Cepheid, the star has featured in just five papers (according to SIMBAD), all providing or regurgitating photometry with not a single spectroscopic observation reported. There appears to be confusion as to whether it is a Type I or II star. Our estimate of the intrinsic $[Fe/H]$ of -0.6 suggests that it is not a Classical Cepheid.

SZ Mon: This Cepheid is not listed by Harris (1985). Apparently, it was assumed to be a Classical Cepheid. This assumption was rejected by Stobie (1970) and Lloyd Evans (1970), largely on the grounds that alternating minima are of different depths. The star is either a W Vir or a RV Tau variable. If the latter description is correct, the fundamental period is approximately 32.6 days. SZ Mon has a marked infrared excess (McAlary & Welch 1986).

W Vir: The prototypical Type II Cepheid with an extensive record of published photometric and spectroscopic observations. As befits the prototype, its composition is broadly representative of the other W Vir stars. Our results are in fair accord with the first results given long ago by Barker et al. (1971).

MZ Cyg: Type II according to Harris (1985) with $|Z|$ of 0.9 kpc. The light curve (Schmidt et al. 2004a) is unlike that of a Classical 21 day Cepheid. Emission in $H\alpha$ and

He I 5876 Å occurring coincident with the bump on the rising light curve is taken to be a discriminant between Type II and Type I Cepheids. Schmidt et al. (2004b) report such emission for MZ Cyg and thus confirm its designation as a Type II Cepheid. The [Fe/H] reminds one of the metal-rich RR Lyraes with Pop. II kinematics.

CC Lyr: Harris (1985) estimated a $|Z|$ of 2.7 kpc and, hence, identified it as a Type II Cepheid. Photometry shows alternating minima of different depths, a characteristic of RV Tau variables (Schmidt et al. 2004a). CC Lyr has a strong infrared excess, also invariably a characteristic of RV Tau variables. This star’s spectrum betrays an obvious signature of dust-gas separation, a mark of warm RV Tau variables. CC Lyr’s spectrum contains few lines, a reflection of the fact that the atmosphere is highly depleted in many elements including Fe. Figure 1 shows C I lines but not the Fe I and Ni I lines seen in spectra of the other three stars. The intrinsic metallicity is about $[A/H] \simeq -0.8$ as indicated by the S and Zn abundances which we assume are undepleted. The measured iron abundance is $[Fe/H] \simeq -4$ which corresponds to a dust-gas depletion of more than three orders of magnitude!

RX Lib: Harris (1985) put RX Lib in his table; the estimated $|Z|$ was 3.2 kpc. Earlier, Harris & Wallerstein (1984) placed RX Lib in a category ‘Stars thought not to be Cepheids’ remarking that the type for this star is ‘uncertain’. Apparently, observations – spectroscopic and photometric – have not been published since the mid-1980s on this star. Although the type may be ‘uncertain’, RX Lib’s composition is similar to that of W Vir.

TW Cap: The metallicity, $[Fe/H] = -1.8$, and essentially a normal composition for a halo star suffice to identify this as a Type II Cepheid. The star’s position in the P-R diagram supports the Type II designation (Böhm-Vitense et al. 1974). Harris (1985) classified the star thus on the basis of its estimated 2 kpc distance from the Galactic plane.

V1711 Sgr: Harris (1985) listed this star as a Population II Cepheid. In the limited literature on V1711 Sgr, there is a lone dissenting voice about the classification. Berdnikov & Szabados (1998) find a difference in amplitude between their light curve and that obtained about two decades earlier by Dean et al. (1977) and suggest that the star may be a SRd variable. Presence of an IR excess (Lloyd Evans 1985; McAlary & Welch 1986; Smith 1998) and a composition bearing the signature of dust-gas separation (see below) together with the long period suggest that the star may be related to the RV Tau variables. We follow Harris and include the star among our sample of Type II Cepheids. The period of 28.56 days reported Berdnikov & Szabados (1998) is adopted and not the 30.5 days listed by Harris (1985).

4. Implications of the Chemical Compositions

4.1. The Evolutionary Context

Type II Cepheids in the instability strip above the horizontal branch have evolved from stars on the blue end of the horizontal branch (BHB) where the stars are He-core burners. Placement of a star on the horizontal branch following evolution to the tip of the first red giant branch requires substantial mass loss by processes as yet unidentified. Seminal calculations about Type II Cepheids were reported by Gingold (1974, 1976, 1977, 1985). Gingold (1985, Figure 1) shows two evolutionary tracks starting from the BHB that may bracket the origins of the Type II Cepheids. Figure 2 is an adaptation of Gingold’s figure. The form of the track appears to depend principally on the mass of the envelope (relative to the core mass) and weakly on the initial metallicity.

In the simpler of the two tracks, the blue horizontal branch star evolves to the red, crosses the instability strip as a BL Her variable, and evolves up the AGB to endure thermal pulses before leaving the AGB tip for rapid evolution to the blue across the instability strip as a RV Tau star and a brief experience as a post-AGB star. We refer to this type of evolution as following a track-direct.

In the alternate path, a star from the more extreme blue part of the BHB evolves to the red, crosses the instability strip to approach the AGB but experiences a structural readjustment between the H and He shell burning shells that directs the evolutionary track back to the blue. The star executes a ‘bluenose’ (Gingold’s parlance) involving two more transits across the instability strip and returns to the AGB from which after increasing in luminosity it can make its final departure across the instability strip to the blue as a post-AGB star. This track makes four crossings of the instability strip: the first three with a period representative of BL Her variables and the final one as a W Vir or RV Tau variable. We refer to this type of evolution as following a track-bluenose.

In both evolutionary tracks, the luminosity difference between the earlier one or three and the final crossings of the instability strip is the key to the period gap in the distribution function of Type II Cepheids between the BL Her and W Vir variables. This distribution necessarily depends on the time taken to transit the instability strip on each crossing (Gingold 1985) and on the rate of production of stars evolving along a track-direct and a track-bluenose.

Metal-rich RR Lyraes discovered by Preston (1959) long posed a puzzle because metal-rich low-mass stars after the He-core flash settle as He-core burning giants to the red of the RR Lyrae gap, the so-called clump giants. A clump He-core burning giant evolves up the

AGB where episodic thermal pulses begin at high luminosity. Such pulses are not predicted to lead to excursions into the instability strip to the blue of the AGB (see Iben 1991 - his Fig. 5 and Gingold 1985 - his Fig. 1). Taam, Kraft, & Suntzeff (1976) proposed that severe mass loss would place giants with a low mass envelope away from the clump and on the horizontal branch in or to the blue of the RR Lyrae gap. Subsequent evolution of these horizontal branch stars produces a metal-rich BL Her or W Vir, as above. Gingold (1977) also showed that even stars placed on the red horizontal branch would, if the envelope mass were reduced sufficiently, evolve first to the blue. Taam et al. showed that kinematically the metal-rich RR Lyraes were members of the old (now, thick) disk.

How thick-disk giants lose the required amount of mass (about $0.5M_{\odot}$ – Taam et al. 1976) and reduce their envelope to a few per cent of a solar mass is unknown. Observers may speculate that the He-core flash that precedes He-core burning may lead in rare but sufficient cases to internal violence and mass loss. This oft-invoked speculation has yet to find a resonance in theoretical calculations – see recent reports by Deupree (1996) and Dearborn, Lattanzio, & Eggleton (2006). In the absence of observationally confirmed theoretical ideas on how severe mass loss is achieved, it is impossible to predict the changes of surface composition expected of BL Her, W Vir, and RR Lyr stars relative to their initial (main sequence) composition. Horizontal branch stars including RR Lyr variables must be affected by the first dredge-up occurring at the base of the red-giant branch and by other subsequent events such as the mass loss required to account for a star’s position on the horizontal branch. Principal effects will be on C, N, and O, possibly He, and certainly Li, Be, and B.

Three BL Her stars in our sample (IX Cas, TX Del, and AU Peg) and the W Vir star ST Pup (Gonzalez & Wallerstein 1996) are known spectroscopic binaries for which previous mass transfer may have directed their primary star to the instability strip. Although other binaries may lurk undetected in the sample, well observed stars like W Vir must, if accompanied by a companion, have a very low velocity amplitude.

4.2. Observed composition and period

The BL Her stars and the W Vir stars occupy different positions along the evolutionary tracks from the blue horizontal branch to the post-AGB departure from the AGB; the BL Her stars are closest to the blue horizontal branch and the W Vir stars are presumed to be leaving the AGB. In light of this difference in staging along the evolutionary tracks, we distinguish the two classes in discussing their compositions.

The BL Her variables are stars with pulsation periods of four days or shorter plus TX

Del and IX Cas, stars of intermediate period but with the signature of BL Her stars, i.e, an overabundance of Na. The BL Her stars have on average a higher $[\text{Fe}/\text{H}]$ than the W Vir stars. The W Vir variables are stars with pulsation periods of greater than about 10 days plus the intermediate period stars AL Vir and AP Her. Among the W Vir stars is CC Lyr which, as noted above, has a composition indicative of severe dust-gas separation, a common feature of RV Tau variables. Other W Vir stars offer indications of dust-gas separation and some have light curves suggestive of RV Tau-like pulsations.

The compositions of the stars are given in Table 2 for the BL Her stars, Table 3 for the intermediate period quartet, and Table 4 for the W Vir stars. In Figures 2 to 5 displaying the results as $[\text{X}/\text{Fe}]$ versus $[\text{Fe}/\text{H}]$, the BL Her stars (including TX Del and IX Cas) are represented by unfilled circles, the W Vir stars (including AL Vir and AP Her) by filled circles. In addition to our sample, we plot the previously published results for the C-rich BL Her stars – V553 Cen (Wallerstein & Gonzalez 1996) and RT TrA (Wallerstein, Matt, & Gonzalez 2000) – as unfilled squares, the W Vir stars ST Pup (Gonzalez & Wallerstein 1996) and κ Pav (Luck & Bond 1989) as filled triangles.

Studies of the kinematics of Type II Cepheids show that the examples in the solar vicinity are primarily thick disk stars with an admixture of halo stars. Initial compositions of thick disk and halo stars are now known as a function of metallicity. The thin and thick disk do not have identical compositions as a function of metallicity (Bensby et al. 2005; Reddy et al. 2006). The differences at a given $[\text{Fe}/\text{H}]$ are not large. Of relevance to our discussion is the fact that at a given $[\text{Fe}/\text{H}]$ the scatter in initial abundance ratios, i.e., $[\text{X}/\text{Fe}]$, is very small for both the thin and the thick disk, at least for the stars now in the solar neighborhood (Edvardsson et al. 1993; Reddy et al. 2003, 2006). At a common low $[\text{Fe}/\text{H}]$, the composition of thick disk and halo stars appear to merge but the scatter in $[\text{X}/\text{Fe}]$ at a given $[\text{Fe}/\text{H}]$ may be more significant for the halo population. Since our sample includes just two halo stars, this scatter in composition, if real, is unimportant here.

The compositions of the variables are judged relative to their presumed initial compositions as inferred (usually) from their $[\text{Fe}/\text{H}]$, but, an alternative is considered in the cases where dust-gas separation is suspected.

4.3. The BL Herculis variables

Our sample is augmented by published analyses of the BL Her C-rich variables V553 Cen and RT TrA.³ Consideration of the C, N, and O abundances led Wallerstein and colleagues to propose that the atmospheres of the two C-rich variables had been enriched in ^{12}C from the 3α -process followed by operation of the H-burning CN-cycle. The high C abundances pointed to the 3α -process. Operation of the CN-cycle was indicated by the high N abundances. Measurement of the $^{12}\text{C}/^{13}\text{C}$ ratio for both stars gave results equal to the equilibrium value for the CN-cycle, an indication that CN-cycling occurred following the ^{12}C enrichment from the 3α -process. A Na enrichment was attributed to proton capture on ^{22}Ne occurring at the time of H-burning. This combined operation of the H-burning CN cycle and the He-burning 3α -process and attendant reactions may account for the BL Her stars analyzed here. (The halo variable UY Eri is not discussed further.)

Prior to a star’s transfer to the horizontal branch, the first dredge-up increased the surface N abundance at the expense of the C abundance. The maximum possible N abundance post dredge-up is obviously equal to the sum of the initial C and N abundances. Oxygen is not predicted to be reduced by the dredge-up. The C and N abundances show clearly that the first dredge-up has not been the primary influence on the stars’ surface abundances. The C abundance for all but one star (IX Cas) equals or exceeds the initial abundance. The N abundance except for IX Cas and DQ And exceeds by about 0.6 dex that predicted by complete conversion of initial C and N to N. The N abundance is approximately that expected by complete conversion of initial C, N, and O to N but the O abundance is not depleted but has an abundance similar to or even slightly greater than the presumed initial abundance. One star – SW Tau – is C-rich with a C/O ratio of about 3. A second – BL Her – is borderline C-rich with C/O of 0.9. With the remarkable exception of IX Cas (C/O = 0.005), SW Tau, and BL Her, the other BL Her stars have a C/O ratio in the range 0.1 to 0.4. The C, N, and O abundances signal the presence of 3α -process and CN-cycle products.

A sodium overabundance is an obvious feature of the eight BL Her variables (Figure 3). The $[\text{Na}/\text{Fe}]$ ratio over the interval $-0.5 < [\text{Fe}/\text{H}] < +0.2$ is independent of $[\text{Fe}/\text{H}]$ with a spread of about 0.5 dex and a mean $[\text{Na}/\text{Fe}] = +0.73$, a substantial increase over the ratio of +0.12 for the thick disk (Reddy et al. 2006). Wallerstein and colleagues obtained a Na overabundance for their pair of C-rich BL Her variables: $[\text{Na}/\text{Fe}] = +0.74$ (RT TrA) and +0.43 (V553 Cen). The mean $[\text{Na}/\text{Fe}]$ for the W Vir stars excluding the halo star TW Cap, and the stars (ST Pup, CC Lyr, and V1711 Sgr) affected by dust-gas separation is $[\text{Na}/\text{Fe}]$

³Other C-rich variables listed by Lloyd Evans (1983) have periods of 20 days or longer. None have been subject to quantitative analysis.

= +0.23, a value consistent with the ratio of unevolved thick disk stars.

The Al abundances of the BL Her stars give a mean $[\text{Al}/\text{Fe}] = +0.13$, a value confirmed by the pair of C-rich variables. The mean $[\text{Al}/\text{Fe}]$ is slightly less than that of thick disk stars for which Reddy et al. (2006) gave $[\text{Al}/\text{Fe}] = +0.30$. The mean $[\text{Na}/\text{Al}]$ of the BL Her stars is +0.60 but the presumed initial ratio for the thick disk stars is -0.18 , a factor six change in the Na/Al ratio occurring in the course of evolution to a BL Her variable. The W Vir stars show a wide range in Al abundance which we attribute to dust-gas separation but the upper limit in the range is consistent with the ratio for thick disk stars.

The α -elements, here Mg, Si, S, Ca, and Ti, conform to expectation. At thick disk metallicities, the ratios $[\alpha/\text{Fe}]$ are positive for the dwarfs: $[\alpha/\text{Fe}] = +0.32$ (Mg), +0.22 (Si), +0.18 (Ca), and 0.21 (Ti) at $[\text{Fe}/\text{H}] \simeq -0.5$ (Reddy et al. 2006). (Sulphur was not examined by Reddy et al. but a value for $[\text{S}/\text{Fe}]$ close to those of Mg and Si is expected.) Thick disk stars with $[\text{Fe}/\text{H}] > -0.3$ have thin disk abundances with a decline of $[\alpha/\text{Fe}]$ to zero at about $[\text{Fe}/\text{H}] = 0$. The observed $[\alpha/\text{Fe}]$ ratios versus $[\text{Fe}/\text{H}]$ are shown in Figure 4. They match expectation well for the composite index from Mg, Si, and S. The observed $[\text{Ca}/\text{Fe}]$ for $[\text{Fe}/\text{H}] < 0$ stars is as expected but for the low $[\text{Ca}/\text{Fe}]$ for AU Peg. AU Peg also shows a low $[\text{Ti}/\text{Fe}]$.

Iron-group abundances (here, Cr, Mn, and Ni) shown in Figure 5 as a function of $[\text{Fe}/\text{H}]$ follow well the trends expected of disk stars (Reddy et al. 2006): $[\text{Cr}/\text{Fe}] \simeq [\text{Ni}/\text{Fe}] \simeq 0$ and $[\text{Mn}/\text{Fe}] \leq 0$. Two of the stars – BX Del and TX Del – appear to be Sc-poor relative to expectation. Both are also Ti-poor. The Zn abundances follow expectation, i.e., $[\text{Zn}/\text{Fe}] \simeq 0$, with the possible exception of DQ And.

Abundances of heavy elements in Type II Cepheids have occasioned considerable comment beginning with Rodgers & Bell’s (1963) analysis of κ Pav where they reported an underabundance by about a factor of seven of s -process elements (relative to the Fe abundance). A new analysis of κ Pav was made by Luck & Bond (1989) who found $[s/\text{Fe}] = -0.4$ at $[\text{Fe}/\text{H}] = 0.0$. The s -process contribution is here compiled as a simple mean of the derived Y, Zr, La, and Ce abundances. Neodymium with roughly equal s - and r -process contributions at the solar composition (Burriss et al. 2000) was not included but its inclusion would not alter any conclusions. The expected $[s/\text{Fe}]$ for the thick disk is close to zero. Figure 6 shows that this expectation is found for five of our seven BL Her variables, and C-rich V553 Cen, and RT TrA. Three BL Her stars – BX Del, VY Pyx, and TX Del – have $[s/\text{Fe}] \simeq -0.5$, a value far from the range shown by thick (and thin) disk unevolved stars. There is a tantalising hint that the $[s/\text{Fe}]$ values offer a bimodal distribution. The low- s stars are discussed further in the next section on the W Vir stars for which underabundance of s -process elements is common.

Europium is taken as the sole measure of the r -process contribution to the stellar composition; Eu in the solar composition is about 97% r -process (Burris et al. 2000).⁴ Europium abundances for the BL Her variables are shown in Figure 7. A tight relation is seen with a tendency for $[\text{Eu}/\text{Fe}]$ to increase with decreasing $[\text{Fe}/\text{H}]$. This relation mimics that for the thick disk but is displaced at a given $[\text{Fe}/\text{H}]$ to lower $[\text{Eu}/\text{Fe}]$ by about 0.2 dex. One presumes that this is an artifact of the analysis and not a consequence of stellar evolution.

Among the W Vir stars, dust-gas separation is unmistakably severe in the case of CC Lyr and suspected in several other cases. The signatures of severe dust-gas separation are $[\text{S}/\text{Fe}]$ and $[\text{Zn}/\text{Fe}]$ ratios in excess of their normal ratios for thick disk stars of about +0.3 and 0.0, respectively, and negative ratios for $[\text{Al}/\text{Fe}]$, $[\text{Sc}/\text{Fe}]$, and $[\text{Ti}/\text{Fe}]$. In mild cases, the effects of separation are limited to the elements of highest condensation temperature (Al, Sc, and Ti) and, then $[\text{Al}/\text{Fe}]$, $[\text{Sc}/\text{Fe}]$, and $[\text{Ti}/\text{Fe}]$ show negative values but $[\text{S}/\text{Fe}]$ and $[\text{Zn}/\text{Fe}]$ have normal values. In our sample of BL Her variables, none show the signature of severe dust-gas separation. The trio with a low $[s/\text{Fe}]$, also a signature of depletion of the highest condensation temperature elements, provide weak hints of depletion of Al, Sc, and Ti.

In summary, the composition of the BL Her variables, as suggested by Wallerstein and colleagues from their analyses of the C-rich pair of variables, has been set by mixing with the products of 3α - processing, CN-cycling, and p -capture on ^{22}Ne . Other abundance ratios relative to Fe have their expected values with the exception of low s -process abundances for a minority of the group.

4.4. The W Virginis Variables

The W Vir stars as a class show evidence in their C, N, and O abundances for the presence of 3α -process and CN-cycle products in their atmosphere but not the Na overabundance seen for the BL Her variables. A signature of weak dust-gas separation seems present in some stars with a clear signature of severe separation present for CC Lyr and ST Pup (Gonzalez & Wallerstein 1996). The sample of W Vir stars has on average a lower (intrinsic) $[\text{Fe}/\text{H}]$ than the sample of BL Her stars.

The first dredge-up is clearly not the defining part of the evolutionary history. For four stars, although the N abundance may be equal to the sum of the initial C and N abundances,

⁴Luck & Bond adopted the mean of their measured elements from La to Eu as an indicator of the r -process. This choice includes La and Ce which in the solar mixtures are about 80% s -process and only 20% r -process.

the C abundance either remains equal to the initial abundance or exceeds it by as much as 0.8 dex. In two cases, the N abundance exceeds the sum of the initial C and N abundances. The C/O ratios range from about 2 for MZ Cyg and SZ Mon to 0.06 for W Vir. Although lacking a counterpart to IX Cas with its low C abundance, the spread in C, N, and O abundances is similar to that of the BL Her variables.

The striking difference in the $[\text{Na}/\text{Fe}]$ ratios of the BL Her and W Vir stars (Figure 3) is a clue to their different origins. Setting ST Pup and V1711 Sgr aside, the $[\text{Na}/\text{Fe}]$ of the W Vir stars appears independent of $[\text{Fe}/\text{H}]$ and pulsation period, and consistent with that found for the thick disk dwarfs but significantly less than that of the BL Her variables. The exceptions, both with the high $[\text{Na}/\text{Fe}]$ representative of the BL Her variables, are ST Pup and V1711 Sgr. ST Pup (Gonzalez & Wallerstein 1996) is seriously affected by dust-gas separation such that neither the present Fe and nor most likely also the Na abundance are unaffected. It is impossible at present to correct the observed $[\text{Na}/\text{Fe}]$ for the effects of dust-gas separation but a downward revision is certain. V1711 Sgr may be a Na-rich W Vir star but distortion of the $[\text{Na}/\text{Fe}]$ ratio by dust-gas separation effects cannot be excluded. Although V1711 Sgr is not as dramatically affected by dust-gas separation as ST Pup, the $[\text{Na}/\text{Fe}]$ may have been increased sufficiently (say, by 0.3 dex) to place it among the BL Her stars.

Aluminum is in the main less abundant in W Vir than in BL Her stars (Figure 3). All W Vir stars show a $[\text{Al}/\text{Fe}]$ less than that of the thick disk dwarfs. ST Pup’s positive $[\text{Al}/\text{Fe}]$ is anomalous for a star strongly affected by dust-gas separation (see below).

Abundances of the α -elements (Figure 4) show a greater spread for $[\text{Ca}/\text{Fe}]$ and $[\text{Ti}/\text{Fe}]$ versus $[\text{Fe}/\text{H}]$ than is the case for the BL Her stars. The spread is greater for $[\text{Ti}/\text{Fe}]$ than for $[\text{Ca}/\text{Fe}]$ and almost absent for $[\text{Mg}/\text{Fe}]$, $[\text{Si}/\text{Fe}]$, and $[\text{S}/\text{Fe}]$. The appearance of negative $[\text{Ca}/\text{Fe}]$ and $[\text{Ti}/\text{Fe}]$ is consistent with the operation of dust-gas separation.

The r -process element Eu defines a similar $[\text{Eu}/\text{Fe}]$ versus $[\text{Fe}/\text{H}]$ relation for the BL Her and W Vir stars which incorporates the two C-rich BL Her stars (Figure 6).

The s -process abundances show apparently bimodal values of $[s/\text{Fe}]$ of about 0.0 or -0.7 , a tendency similar to that provided by the BL Her stars. Given that $[s/\text{Fe}] \simeq 0.0$ is representative of the thick disk, the anomalous stars are those with negative $[s/\text{Fe}]$ values. As noted above, the s -poor stars have negative $[\text{Ti}/\text{Fe}]$ and not the positive values expected of thick disk stars and negative $[\text{Sc}/\text{Fe}]$ with values of about -1 in four cases. (The W Vir star κ Pav, as analysed by Luck & Bond (1989), is a typical s -process deficient member of the class.)

Longer-period W Vir stars and shorter-period RV Tau stars overlap in period and,

therefore, it of interest to comment on similarities and differences in composition. The C, N, and O abundances of the two groups have very similar ranges and mean values (Giridhar et al. 2005). Of especial interest in the [Na/Fe] ratio of RV Tau stars. Since many RV Tau stars show a Fe-depletion from dust-gas separation, we compare not [Na/Fe] but [Na/Zn] because Zn is generally not depleted and [Zn/Fe] $\simeq 0$ in unevolved stars. We compile [Na/Zn] for RV Tau stars from results given by Giridhar et al. (2005) and earlier papers in that series. The mean value from 21 stars is [Na/Zn] = $+0.17 \pm 0.03$ to be compared with [Na/Zn] = $+0.20$ for our W Vir stars and $+0.85$ for our BL Her stars. Excluded from our sample of RV Tau stars are two stars with the high [Na/Zn] characteristic of the BL Her stars, CE Vir where the abundance anomalies are not due to dust-gas separation (Rao & Reddy 2005), and EP Lyr where the dust-gas separation is so severe that Na is somewhat depleted. The conclusions are that the distribution of [Na/Zn] ratios (i.e., the [Na/Fe] in the absence of dust-gas separation) of the W Vir and the RV Tau stars are identical with the majority showing no sodium enrichment but a minority of perhaps 10 per cent showing the sodium enrichment of the BL Her stars.

4.5. Accounting for the anomalies

Introduction to the stellar surface of products of internal nucleosynthesis is a well known phenomenon accounting in principle for a surface composition differing from the presumed initial composition. The classic case must be that of those S stars with Tc present at the surface. The qualifying phrase ‘in principle’ recognises that the details of the internal nucleosynthesis and dredge up to the surface may not yet be understood. Often, the particular processes of nucleosynthesis involved are identifiable and it is the modes of transport of the nucleosynthetic products to the atmosphere that are in doubt.

Such would appear to be the case for the BL Her stars. The atmospheres are contaminated, as Wallerstein and colleagues first showed from their analyses of two C-rich BL Her stars, with 3α -processed material followed by exposure to the CN-cycle. This recipe which accounts in principle for the C, N, O, and Na abundances of the BL Her stars has yet to be incorporated into a stellar evolution model that ties the nucleosynthesis and mixing to events in the life of a low-mass star. The sole remaining abundance anomaly is the appearance of a low [s/Fe] in three stars. There are hints of anomalously low Ca, Ti, and Sc in a minority. Such hints lack an obvious nucleosynthetic explanation, even in principle.

In searching for the origin of the abundance anomalies of the Population II Cepheids, one may begin with the Na abundance difference between the W Vir and BL Her stars. Recall that the W Vir stars are considered to have evolved from BL Her stars. Sodium destruction

is highly unlikely to have occurred along the track between the BL Her and W Vir phases. Thus, it seems clear that the W Vir stars observed here cannot be direct descendants of the BL Her stars observed here; V1711 Sgr may be an exception. Since, sodium production is highly unlikely to be a feature of the short evolutionary phase from the BHB to the instability strip, the overabundance of sodium in BL Her stars must be attributed to the as yet unknown processes involving mixing and mass loss that placed the BL Her progenitors on the BHB. Continuing this thought we conjecture that the processes which placed the W Vir progenitors on the BHB did not provide for a sodium overabundance. The unknown processes in both cases involved 3α -process and the CNO-cycles to similar degrees. Given that the distributions of C, N, and O abundances are similar for BL Her and W Vir stars, the difference involving the unknown processes would appear to have been the temperature at which the CNO-cycles operated. Sodium production by proton capture on ^{22}Ne occurs at ‘high’ but not at ‘low’ temperatures. We speculate that mixing and mass loss involving CNO-cycling at high temperatures placed the star near the red end on the BHB with the star evolving along a track-direct to become a Na-rich BL Her star. When CNO-cycling at low temperatures was involved, the star was deposited at the blue end of the BHB. This disposition of progenitors along the BHB and evolution of BHB stars to BL Her and W Vir stars is discussed further in Section 6.

The anomalies common among W Vir stars but uncommon among BL Her stars are very unlikely to have a nucleosynthetic origin. Anomalies include the low $[\text{Al}/\text{Fe}]$, $[\text{Ca}/\text{Fe}]$, $[\text{Sc}/\text{Fe}]$, $[\text{Ti}/\text{Fe}]$, and $[s/\text{Fe}]$ ratios. A catalog of explanations for the anomalies includes the standard invocation of errors in the atmospheric parameters, non-LTE effects, the inapplicability of standard atmospheres invoking hydrostatic equilibrium to a low density atmosphere subject to a pulsation, non-LTE overionization of atoms and ions by Lyman continuum photons from a shock wave in the pulsating atmosphere, substantial helium enrichment leading to a systematic overestimate of (say) $[\text{Fe}/\text{H}]$ but to small(er) effects on ratios such as $[s/\text{Fe}]$, and reduction of the abundance of refractory elements by dust-gas separation in the upper atmosphere or in a circumbinary disk.

Luck & Bond (1989) showed that errors in the atmospheric parameters cannot erase the low $[s/\text{Fe}]$ values, and by extension of their arguments, other anomalous underabundances (relative to Fe) cannot be attributed to injudicious choices of atmospheric parameters. Non-LTE effects computed for standard atmospheres deserve examination but are unlikely to account for example for differences in abundance anomalies between and within the samples of BL Her and W Vir variables where stars of similar atmospheric parameters can differ in the degree of their anomalies.

The possibility of Lyman continuum emission leading to departures from LTE ionization

equilibrium was mentioned by Barker et al. (1971) following a suggestion by Wallerstein, and discussed in more detail by Luck & Bond (1989). Since the observable heavy elements from Y to Eu are present in these atmospheres predominantly as singly-charged ions, all with ionization potentials less than ionization potential of H, the idea has an appeal. Emission in Balmer H α and the He I 5876 Å lines is a feature of the rising branch for the longer-period Type II Cepheids for which *s*-process and other underabundances are common. The fact that Eu does not show an abundance scatter like the *s*-process elements is a strike against the proposal. It also does not account for the underabundance of Al; Al⁺ has an ionization potential of 18.83 eV and Lyman emission at 18.8 eV must be weak and, certainly, Mg present in the atmosphere as Mg⁺ with an ionization potential of 15.04 eV is never underabundant. The idea might be given a stringent test by observing a star at intervals throughout its pulsation and seeing if the derived composition correlates with the presence of a shock as revealed by line splitting. The weight of the evidence is that emission from the shock wave is not a major source of the abundance anomalies.

Addition of extensive amounts of 3 α -processed and CN-cycled material might foster the idea that the reported abundance anomalies are a consequence of analysing the spectrum of a He-rich atmosphere on the assumption that it has a normal He abundance. To first order, this incorrect assumption results in [X/Fe] ratios close to the actual values but a [Fe/H] that is overestimated. Luck & Bond (1989) speculated that a low [*s*/Fe] ratio, a feature of normal stars of [Fe/H] < -2, was being associated with a higher [Fe/H] because of an overlooked helium enrichment. The reader is referred to their paper for arguments leading to the conjecture’s rejection. Here, we note their point that the kinematics of the W Vir stars show that they belong to the thick disk and not to the very metal-poor halo. Yet, a thorough attempt to measure the He/H ratio of the metal-rich variables would be welcomed.

Dust-gas separation is evident in RV Tau variables (Giridhar et al. 2005; Maas, Van Winckel, & Waelkens 2002) except for the metal-poor and cool variables. In oxygen-rich gas, the heavy elements are among the first to be removed from the gas as cooling occurs. The demonstration by Alcock et al. (1998) that the RV Tau and Type II Cepheids in the LMC define a single period-luminosity-color relation suggests that the longer period Type II Cepheids in our sample may be susceptible to dust-gas separation. Earlier, we noted that several of our stars show RV Tau-like photometric behavior and might be promoted from W Vir to RV Tau status. The signature of dust-gas separation, previously reported for ST Pup (Gonzalez & Wallerstein 1996), is strikingly evident here for CC Lyr where the spectrum contains lines of elements having a low condensation temperature (T_C), i.e., lines of C I, N I, O I, Na I, S I, and Zn I, but lines of higher condensation temperature are poorly represented or not detected at all. Severe underabundances are measured, e.g., [Mg/H] \simeq [Fe/H] \simeq -4 but [S/H] \simeq [Zn/H] \simeq -0.5. Figure 7 constructed for CC Lyr shows the

characteristic pattern for a strongly affected RV Tau variable; the abundances $[X/H]$ decline smoothly with increasing condensation temperature. The Mg and Fe deficiencies of CC Lyr are more extreme than any reported previously for a RV Tau variable. Lines of the elements normally the most depleted – Al, Ca, Sc, and Ti, for example – could not be detected in our spectra. CC Lyr has a considerable infrared excess from circumstellar dust. Its Fe deficiency is typical of values reached in the warm post-AGB stars known to be spectroscopic binaries (Van Winckel, Waelkens, & Waters 1995). One supposes that CC Lyr may also be a spectroscopic binary. ST Pup, a W Vir star with a strong infrared excess and signatures of dust-gas separation, was shown by Gonzalez & Wallerstein (1996) to be a spectroscopic binary with an orbital period of 410 days.⁵

The signature of dust-gas separation seems present in other W Vir stars, all of which show negative $[Sc/Fe]$ values. Since these stars are likely thick-disk members of different initial $[Fe/H]$, we correct the derived abundances $[X/H]$ for the initial $[X/H]$ of the thick disk (Reddy et al. 2006) before presenting the T_C versus $[X/H]$ plots; all corrections are small. Figure 8 shows the $[X/H]$ versus T_C plots for CO Pup and W Vir. In such cases, as in the examples of mildly affected RV Tau stars, the scatter in $[X/H]$ at a given condensation temperature may be significant. This scatter is attributed to the understandable failure of the condensation temperature to represent fully the complex processes of dust formation and accretion of gas but not dust by the star. The decrease in $[X/H]$ at the highest T_C is clear for CO Pup. For W Vir, this signature of dust-gas separation is critically dependent on the Sc abundance. Here and in Figures 9 and 10, the s -process elements are denoted by unfilled circles. Lack of a clear separation between the unfilled and filled circles referring to elements of similar T_C show that the s -process products did not mix to the surface in the time that these W Vir stars were on the AGB. A clearer example of dust-gas separation is provided by V1711 Sgr with Al, Ti, and Sc, all underabundant by more than one dex relative to Fe (Figure 9). The signature of dust-gas separation also seems evident for SZ Mon, the W Vir star with a RV Tau-like light curve and a strong infrared excess (Figure 9). The evidence seems fair for MZ Cyg but weaker for RX Lib (Figure 10) where it relies on the low Sc abundance. In all cases, the s -process elements are underabundant, as expected when Al, Sc, and Ti are underabundant. Although several key elements have not been measured for TW Cap, a halo star, the indication is that dust-gas separation has not affected this star; Ca, Ti, Sc, and s -process elements have the abundances expected of a star with $[Fe/H]$

⁵The dust-gas signatures for ST Pup are rather ragged but this is possibly attributable to larger than normal uncertainties in the derived abundances resulting from the very few lines available for most of the elements: $[Fe/H] = -1.47$ with $[S/Fe] = +1.29$ and $[Zn/Fe] = +1.41$ are customary markers of severe dust-gas separation but $[Al/Fe] = +0.19$ is not.

–1.8, a result anticipated from our previous reports on the absence of dust-gas separation in intrinsically metal-poor RV Tau variables (Giridhar et al. 2005).

Binarity has been advanced as a principal key to the dust-gas separation exhibited by RV Tau stars; Van Winckel (2003) suggested that ‘binarity may very well be a common phenomenon among RV Tau stars’. In the present sample, the known spectroscopic binaries – TX Del, IX Cas, and AU Peg – are not strongly affected by dust-gas separation but all are BL Her stars for which dust-gas separation is not observed. The affected W Vir star ST Pup is a binary (Gonzalez & Wallerstein 1996). Investigating the binary nature of the W Vir stars, not only those affected by dust-gas separation, will call for intensive radial velocity monitoring in order to resolve the orbital from the pulsational velocity variations. It is noteworthy that the Fe-deficiency of CC Lyr is similar to that of the A-type post-AGB stars, all known to be spectroscopic binaries (Van Winckel et al. 1995).

In short, the suggestion is clear: the principal reason for the various abundance anomalies – C, N, and O apart – among the W Vir stars is that their atmospheres have been partially cleansed of refractory elements. The mass of the convective envelope must be small to sustain a large deficiency of refractory elements. Perhaps, not coincidentally a small envelope is also a condition required to place the immediate progenitors of these variables on the horizontal branch to the blue of the red clump. There may also be a correlation between the magnitude of the infrared excess and the visibility of the dust-gas separation. Stars with a weak dust-gas separation are returning to a normal composition following dissolution of circumstellar dust. The BL Her stars have yet to evolve to the upper AGB and to commence dust production and, hence, absence of evidence of dust-gas separation is not surprising.

In discussing the abundance anomalies, we have overlooked the possibility that a contributing factor might be found in conditions existing in the progenitors resident on the blue horizontal branch. Stars with the lowest ratios of envelope to core mass reside on the horizontal branch at effective temperatures ($T_{\text{eff}} > 11500$ K) such that severe atmospheric abundance anomalies are created by gravitational settling and radiative levitation (Behr 2003), e.g., Fe overabundances by a factor of 2 dex have been recorded. These stars are likely to evolve along a track-blunose. However, one supposes that such anomalies are erased by the time that the stars have evolved off the horizontal branch and into the instability strip. This supposition deserves observational and theoretical attention.

5. Metallicities from photometry

Accumulation and analysis of high-resolution spectra is a time consuming process. A variety of statistical properties of the Type II Cepheids may be more readily examined using a photometric estimate of metallicity provided that the estimate is reliable. Here, we assess the reliability for three photometric systems which have been applied to Type II Cepheids.

Harris (1981) used Washington photometry to obtain the metallicity $[A/H]$ for a large sample of Type II Cepheids – see Harris & Wallerstein (1984) for two revisions. There are 13 stars not including CC Lyr in common with our sample. The comparison of our $[Fe/H]$ and $[A/H]$ is shown in Figure 11. (The $[A/H]$ for CC Lyr with its highly non-standard composition is expected to depart appreciably from the spectroscopic $[Fe/H]$: indeed, $[A/H]$ of -2.2 versus $[Fe/H]$ of about -4 .) It is clear from the figure that the photometric and spectroscopic estimates are well correlated but offset such that $[A/H]$ is overestimated by about 0.5 dex. The offset is not dependent on the pulsation period of the star. The conclusion is that the Washington photometry provides, after a 0.5 dex downward revision, metallicity estimates of satisfactory quality for statistical purposes – see, for example, the distribution functions for metallicity of Type II Cepheid (Harris 1981).

Diethelm (1990) used Walraven *VBLUW* photometry to estimate the metallicity of the shorter period Type II Cepheids. Five stars are in common with our sample including a RR Lyrae IK Hya (not discussed here). Again, there is an offset between photometric and spectroscopic estimates: $[A/H]$ is overestimated by about 0.5 dex for the metal-rich stars and possibly by 0.8 dex at low $[Fe/H]$ (Figure 11).

Strömgren photometry was applied by Meakes, Wallerstein, & Opalko (1991). Excluding CC Lyr ($[A/H]$ of -2.3), the common stars show that $[A/H]$ and $[Fe/H]$ are roughly correlated (Figure 11).

In summary, the metallicities may be reliably provided by photometry except for stars seriously affected by dust-gas separation.

6. Concluding remarks

Our sample of field Type II Cepheids is the first for which extensive data on chemical compositions are provided. The study complements prior modern analyses of κ Pav, ST Pup, V553 Cen, and RT TrA. Our data on just two halo (metal-poor) Type II Cepheids omit key elements – e.g., C, N, and Na – so that no more than a perfunctory interpretation of these stars is offered. Common to the BL Her and W Vir stars is evidence for addition

to their atmospheres of 3α -processed and CN-cycled material. The distinguishing mark of the BL Her stars, the shorter period Type II Cepheids, is their overabundance of Na, an overabundance not detected among the W Vir stars. The distinguishing mark of the W Vir stars, the longer period Type II Cepheids, is a composition modified by dust-gas separation to varying degrees.

Our following discussion assumes that the post-BHB evolution follows the lines given in Section 4.1 (Figure 2): evolution follows either a track-direct or a track-bluenose and the order of development is BHB \rightarrow BL Her \rightarrow W Vir \rightarrow post-AGB. Then, there are two evolutionary puzzles presented by these distinguishing marks:

1: BL Her stars are Na-rich and evolve to become W Vir stars but none of the analysed W Vir stars with the possible exception of V1711 Sg are Na-rich.

2. W Vir stars have normal sodium abundances and have evolved from BL Her stars but all of the analysed BL Her stars are Na-rich.

In the case of the first puzzle, the simplest explanation is that a long-period (W Vir or RV Tau) variable resulting from a Na-rich BL Her star transits the instability strip much faster than the W Vir star of normal Na abundance. Our discussion of Na abundances of RV Tau stars showed that BL Her-like Na overabundances are seen in approximately 10 per cent of the sample. If V1711 Sgr is Na-rich, a similar fraction of our sample of ten W Vir stars is Na-rich.

Possible resolution of the second puzzle starts with the conjecture that changes to the sodium abundance are determined prior to residence on the BHB by events associated with the mass loss (and mixing) required to divert the star from the red clump to the BHB. Sodium production by proton capture on ^{22}Ne occurs in association with H-burning by the CNO-cycles only at ‘high’ temperatures. Thus, the BHB may be populated by Na-rich and Na-normal stars. Stars deposited on the BHB without experiencing sodium enrichment evolve to Na-normal BL Her stars before becoming Na-normal W Vir stars. The fact that our sample of nine BL Her stars does not include a Na-normal star may be a consequence of a lower production rate of Na-normal to Na-rich BHB stars, and a more rapid crossing of the instability strip by the Na-normal than the Na-rich BL Her stars. Given that a star on a track-bluenose makes three crossings of the instability strip at a period appropriate for a BL Her star, we identify the Na-rich BL Her stars with these tracks. These tracks begin at the blue end of the BHB. The stars on a track-direct start at the red end of the BHB, cross the instability strip once as a BL Her star and then evolve up the AGB to enjoy thermal pulses before entering the instability strip as a W Vir or RV Tau star. Such BHB stars are presumed to lack a sodium enrichment. Examination of a larger sample of BL Her stars is,

then, expected to provide an example or two of a Na-rich variable.

In seeking to resolve puzzles in stellar evolution, one endeavors to connect the stars with their progenitors, descendants, and close relatives among field and cluster stars. The vast majority of our sample are probably thick disk citizens. Close relatives are the RR Lyrae stars at one extreme and RV Tau and post-AGB stars at the other extreme. We have already noted similarities between the compositions of the W Vir and RV Tau stars. Progenitors of the BL Her and W Vir stars are on the blue horizontal branch. Identified BHB stars have halo kinematics and metallicities and are surely progenitors of very metal-poor variables such as UY Eri and TW Cap. Thick disk BHB stars have proven elusive: ‘There are, however, *disk* RR Lyrae stars in the nearby field, but there are (as far as we know) no corresponding field BHB stars that have disk kinematics’ (Kinman et al. 2000). It would be extremely valuable to locate some thick disk BHB stars and to determine their compositions, especially their Na abundances. Our attribution of BL Her stars to a track-bluenose and W Vir stars to a track-direct implies the redder BHB stars should have a normal Na abundance and the bluer BHB stars should be sodium rich.

Fresh insights into the phenomenon of the Type II Cepheids may be gleaned from abundance analyses of these variables in globular clusters. Published results apply to W Vir or RV Tau stars (i.e., periods greater than 10 days) in four globular clusters and five post-HB stars including three variables in ω Cen (cf. Wallerstein’s [2002] review). All variables bar one in ω Cen have a period representative of W Vir stars and the exception with a period of 4.5 days is likely a BL Her star. Results for the globular clusters M2, M5, M10, M12, and M28 – one from each cluster with the exception of two from M5 – are provided variously by Gonzalez & Lambert (1997), Carney et al. (1998), and Klochkova et al. (2003). Gonzalez & Wallerstein (1994) give abundances for the ω Cen stars. The clusters have metallicities from $[\text{Fe}/\text{H}]$ of -1.2 to -1.7 with the stars from ω Cen spanning the range from -1.7 to -2.1 . Thus, the sample is collectively more metal-poor than the large majority of the variables discussed in this paper.

Perhaps, the most significant conclusion to be drawn from these metal-poor stars is that there is no evidence that their atmospheres have been affected by dust-gas separation, a result expected from observations of metal-poor field RV Tau stars (Giridhar et al. 2005). Interpretation of light element abundances (C to Al) is complicated by the fact that many clusters show star-to-star correlated abundance variations that are entirely missing from samples of field stars. Since such variations are present among main sequence members of a cluster, they cannot be explained wholly as internal processing and mixing. In this respect, Carney et al. (1998) show that the variable V42 in M5 has the Na enrichment and O deficiency seen in the most extreme Na-rich and O-poor red giants, i.e., the Na

and O abundances of V42 may be unrelated to its transition from the red giant to the horizontal branch. Notwithstanding this novel complication presented by the clusters and their variables, the preliminary forays into abundance analyses of cluster Type II Cepheids and their horizontal branch progenitors deserve to be extended: for example, the key elements of C, N, and O remain almost untouched by the published analyses (see Gonzalez & Wallerstein for C, N, and O among ω Cen stars, and Klochkova et al. (2003) for C, N, and O for V1 in M12).⁶ Extension of the work on cluster variables to the BL Her stars would also be of interest. This would be of special interest if these BL Her stars are shown to be Na-rich. Material rich in Na from proton capture on ^{22}Ne is possibly also He-rich. The pulsational properties of Type II Cepheids are dependent on the He abundance as well as mass and metallicity (see Bono et al. [1997] for references to these dependencies). Since BL Her stars in globular clusters have an accurately determined absolute luminosity in contrast to field stars where the luminosity is never well determined, it may be possible to determine their helium abundance.

Immediate descendants of the Type II Cepheids are red giants and must be picked out from the (presumably) more numerous giant stars evolved from clump giants. Anomalous compositions are a likely indicator. Wallerstein & Gonzalez (1996) and Wallerstein et al. (2000) noted the similarities between the compositions of the C-rich Type II Cepheids and the R-type carbon stars (Dominy 1984) where products of the 3α -process are greatly in evidence. At the other extreme, IX Cas and the Weak G-band giants may be related examples of stars where the stellar atmosphere is dominated by CNO-cycled products and 3α -processed products are absent or just a minor contaminant. Although intriguing, these suggested links between Type II Cepheids and peculiar red giants do not directly suggest an interpretation in terms of stellar evolution. The observers' *Deus ex machina* for linking a Type II Cepheid to a peculiar red giant may be the He-core flash but, as noted earlier, theoreticians discount this possibility. Perhaps, the appeal should be not to an episode in the life of a single star but to one in the evolution of a binary star. Such an appeal, however, may be a forlorn one in the case of the R-type carbon stars and Weak G-band giants because neither class seem to have an unusual degree of binarity (Tomkin, Sneden, & Cottrell 1984; McClure 1985).

We thank Ron Wilhelm for helpful correspondence. This research has made use of NASA's Astrophysics Data System and the Centre de Données de Strasbourg's SIMBAD

⁶A remarkable result concerns the Al abundance in the ω Cen stars. In four of the five stars, Al was underabundant by -0.3 to -1.1 as measured by $[\text{Al}/\text{Fe}]$ but without the attendant Ca and Sc deficiencies expected from dust-gas separation. Yet more remarkable is the observation that in the fifth star, Gonzalez & Wallerstein (1994) found a strong Al overabundance ($[\text{Al}/\text{Fe}] = +1.2$) in an O-deficient star with a normal Na abundance.

astronomical database. We also thank the anonymous referee for valuable suggestions. This research has been supported in part by the Robert A. Welch Foundation of Houston, Texas.

REFERENCES

- Alcock, C., Allsman, R.A., Alves, D.R., et al. 1998, *AJ*, 115, 1921
- Anderson, K.S., & Kraft, R.P. 1971, *ApJ*, 167, 119
- Andrievsky, S.M., Kovtyukh, V.V., Luck, R.E., et al. 2002, *A&A*, 381, 32
- Asplund, M., Grevesse, N., & Sauval, A.J. 2005, *ASP Conf. Ser.*, 336, 25
- Balog, Z., Vinkó, J., & Kaszás, G. 1997, *AJ*, 113, 1833
- Barker, T., Baumgart, L.D., Butler, D., et al. 1971, *ApJ*, 165, 67
- Behr, B.B. 2003, *ApJS*, 149, 67
- Bensby, T., Feltzing, S., & Lundström, I. 2005, *A&A*, 433, 185
- Berdnikov, L.N., & Szabados, L. 1998, *AcA*, 48, 763
- Böhm-Vitense, E., Szkody, P., Wallerstein, G. 1974, *ApJ*, 194, 125
- Bono, G., Caputo, F., & Santolamazza, P. 1997, *A&A*, 317, 171
- Burris, D.L., Pilachowski, C.A., Armandroff, T.E., Sneden, C., Cowan, J.J., & Roe, H. 2000, *ApJ*, 544, 302
- Caldwell, C.N., & Butler, D. 1978, *AJ*, 83, 1190
- Carney, B., Fry, A.M., & Gonzalez, G. 1998, *AJ*, 116, 2984
- Dean, J.F., Cousins, A.W.F., Bywater, R.A., & Warren, P.R. 1977, *Mem. RAS*, 83, 69
- Dearborn, D.S.P., Lattanzio, J.C., & Eggleton, P.P. 2006, *ApJ*, 639, 405
- Deupree, R.G. 1996, *ApJ*, 471, 377
- Diethelm, R. 1990, *A&A*, 239, 186
- Dominy, J.F. 1984, *ApJS*, 55, 27
- Edvardsson, B., Andersen, J., Gustafsson, B., Lambert, D.L., Nissen, P.E., & Tomkin, J. 1993, *A&A*, 275, 101
- Gingold, R.A. 1974, *ApJ*, 193, 177
- Gingold, R.A. 1976, *ApJ*, 204, 116
- Gingold, R.A. 1977, *MNRAS*, 178, 533

- Gingold, R.A. 1985, *Mem. Soc. Astron. Italiana*, 56, 169
- Giridhar, S., Lambert, D.L., Reddy, B.E., Gonzalez, G., & Yong, D. 2005, *ApJ*, 627, 432
- Gonzalez, G., & Wallerstein, G. 1994, *AJ*, 108, 1325
- Gonzalez, G. & Wallerstein, G. 1996, *MNRAS*, 280, 515
- Gonzalez, G., & Lambert, D.L. 1997, *AJ*, 114, 341
- Harris, H.C. 1981, *AJ*, 86, 719
- Harris, H.C. 1985, *AJ*, 90, 756
- Harris, H.C., Olzewski, E.W., & Wallerstein, G. 1984, *AJ*, 89, 119
- Harris, H.C., & Wallerstein, G. 1984, *AJ*, 89, 379
- Harris, H.C., & Welch, D.L. 1989, *AJ*, 98, 981
- Iben, I. Jr. 1991, *ApJS*, 76, 55
- Kinman, T., Castelli, F., Cacciari, C. et al. 2000, *A&A*, 364, 102
- Klochkova, V.G., Panchuk, V.E., Tavolgenskaya, N.S., & Kovtyukh, V.V. 2003, *Astr. Letters*, 29, 748
- Kraft, R.P. 1972, *Dudley Obs. Rept*, No. 4, 69
- Lloyd Evans, T. 1970, *Obs*, 90, 254
- Lloyd Evans, T. 1983, *Obs*, 103, 276
- Lloyd Evans, T. 1985, *MNRAS*, 217, 493
- Luck, R.E., & Bond, H.E. 1989, *ApJ*, 342, 476
- Maas, T., Van Winckel, H., & Waelkens, C. 2002, *A&A*, 386, 504
- McAlary, C.W., & Welch, D.L. 1986, *AJ*, 91, 1209
- McClure, R.D. 1985, *JRASC*, 79, 277
- McWilliam, A. 1997, *ARAA*, 35, 503
- Meakes, M., Wallerstein, G., & Opalko, J.F. 1991, *AJ*, 101, 1795
- Preston, G.W. 1959, *ApJ*, 130, 507
- Rao, N.K., & Reddy, B.E. 2005, *MNRAS*, 357, 235
- Reddy, B.E., Lambert, D.L., & Allende Prieto, C. 2006, *MNRAS*, 367, 1329
- Reddy, B.E., Tomkin, J., Lambert, D.L., & Allende Prieto, C. 2003, *MNRAS*, 340, 304
- Rodgers, A.W., & Bell, R.A. 1963, *MNRAS*, 125, 487

- Rodgers, A.W., & Bell, R.A. 1968, MNRAS, 139, 175
- Sanwal, N.N., & Sarma, M.B.K. 1991, JAA, 12, 119
- Schmidt, E.G., Johnston, D., Langan, S., & Lee, K.M. 2004a, AJ, 128, 1748
- Schmidt, E.G., Johnston, D., Langan, S., & Lee, K.M. 2005, AJ, 130, 832
- Schmidt, E.G., Johnston, D., Lee, K.M., & Langan, S. 2004b, AJ, 1288, 2988
- Smith, G.H. 1998, PASP, 110, 1119
- Snedden, C., Lambert, D.L., Tomkin, J., & Peterson, R.C. 1978, ApJ, 222, 585
- Stobie, R.S. 1970, MNRAS, 148, 1
- Taam, R.E., Kraft, R.P., & Suntzeff, N. 1976, ApJ, 204, 842
- Tomkin, J., Sneden, C., & Cottrell, P.L. 1984, PASP, 96, 609
- Tull, R.G., MacQueen, P.J., Sneden, C., & Lambert, D.L. 1995, PASP, 107, 251
- Van Winckel, H. 2003, ARAA, 41, 391
- Van Winckel, H., Waelkens, C., & Waters, L.B.F.M. 1995, A&A, 293, L25
- Vinkó, J., Ramage Evans, N., Kiss, L., & Szabados, L. 1998, MNRAS, 296, 824
- Vinkó, J., Szabados, L., Szatmáry, K. 1993, A&A, 279, 410
- Wallerstein, G. 2002, PASP, 114, 689
- Wallerstein, G., & Gonzalez, G. 1996, MNRAS, 282, 1236
- Wallerstein, G., Matt, S., Gonzalez, G. 2000, MNRAS, 311, 414

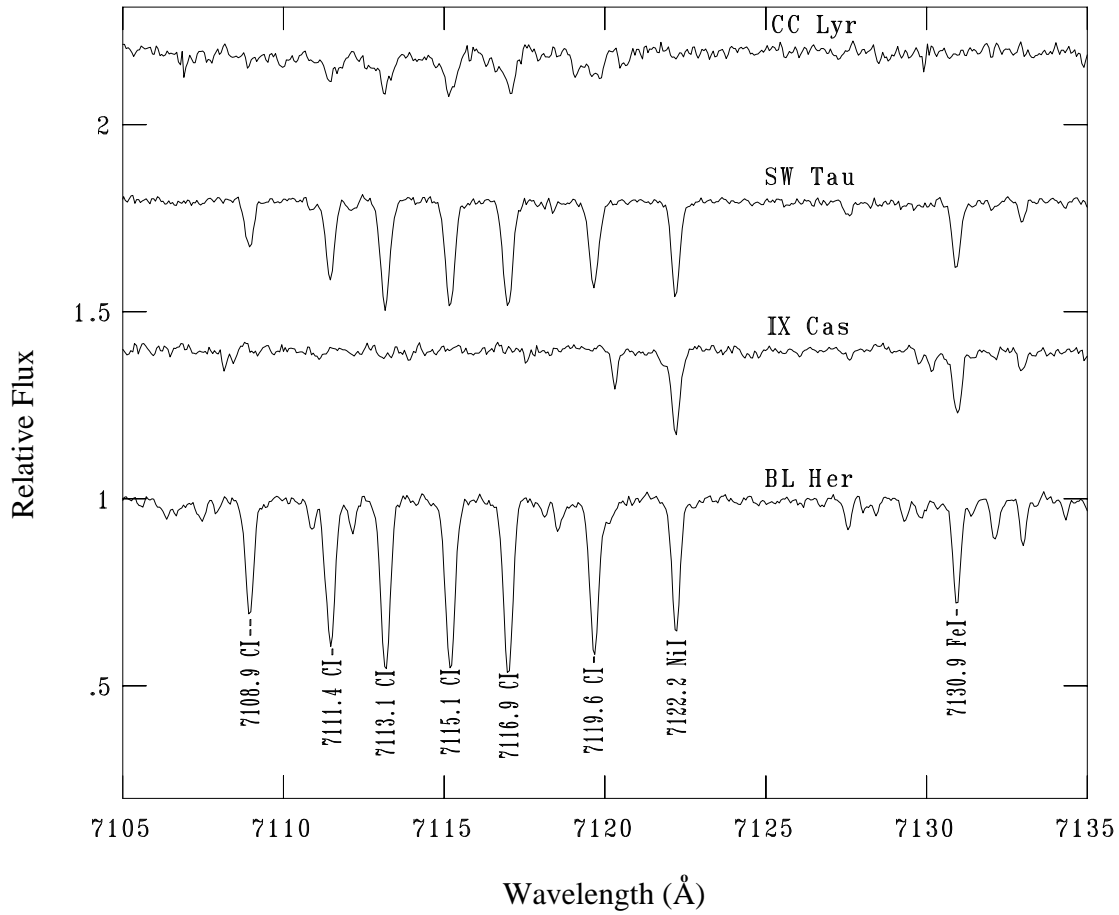


Fig. 1.— The interval 7105–7135 Å for CC Lyr, SW Tau, IX Cas, and BL Her. Note the absence of the C I lines for IX Cas, and the absence of the Fe I and Ni I lines for CC Lyr.

Fig. 2.— A HR diagram showing the location of the Population II instability strip and approximate lines of constant period. Superimposed are two evolutionary tracks for two stars: the track for the $0.6M_{\odot}$ star is a track-direct and that for the $0.536M_{\odot}$ is a track-bluenose (see text). The location of the RR Lyr variables and the approximate positions of RV Tau variables are marked. (After Gingold 1985)

Table 1: STELLAR PARAMETERS FROM THE Fe-LINE ANALYSIS

Star	Period (days)	UT Date	Model		ξ_t^b (km s^{-1})	Fe I ^c		Fe II ^c	
			T_{eff} , log g, [Fe/H] ^a			log ϵ	n	log ϵ	n
BX Del	1.1	2005 Jul 3	6250, 1.0, -0.2		3.0	7.28 ± 0.16	99	7.19 ± 0.19	24
VY Pyx	1.2	2005 Jan 1	5750, 1.5, -0.4		3.0	7.05 ± 0.13	76	6.97 ± 0.14	12
BL Her	1.3	2005 May 3	6500, 2.0, -0.1		2.5	7.32 ± 0.11	122	7.30 ± 0.13	38
SW Tau	1.6	2004 Oct 8	6250, 2.0, +0.2		3.0	7.69 ± 0.12	115	7.66 ± 0.19	24
UY Eri	2.2	2004 Dec 18	6000, 1.5, -1.8		2.9	5.66 ± 0.15	79	5.59 ± 0.10	17
AU Peg	2.4	2005 Sept 24	5750, 1.5, -0.2		5.3	7.26 ± 0.16	37	7.24 ± 0.15	11
DQ And	3.2	2004 Dec 19	5500, 1.5, -0.5		3.0	7.00 ± 0.16	91	7.00 ± 0.13	15
TX Del	6.2	2004 Aug 9	5500, 0.5, +0.1		3.7	7.56 ± 0.09	59	7.56 ± 0.17	16
IX Cas	9.2	2004 Oct 09	6250, 1.0, -0.4		3.3	6.97 ± 0.11	108	6.93 ± 0.14	35
AL Vir	10.3	2004 May 3	5500, 1.0, -0.4		3.5	7.07 ± 0.09	85	7.04 ± 0.13	27
		2005 Jan 30	6500, 1.5, -0.4		3.2	7.04 ± 0.10	92	7.01 ± 0.12	24
AP Her	10.4	2004 Nov 8	6500, 1.0, -0.7		2.7	6.70 ± 0.11	103	6.65 ± 0.17	36
CO Pup	16.0	2004 Dec 19	5000, 0.5, -0.6		4.3	6.81 ± 0.14	130	6.88 ± 0.16	12
SZ Mon	16.3	2005 Jan 30	4700, 0.0, -0.4		3.7	7.02 ± 0.16	59	6.95 ± 0.09	8
W Vir	17.3	2005 Dec 18	5000, 0.0, -1.0		3.8	6.48 ± 0.13	110	6.53 ± 0.13	21
MZ Cyg	21.4	2005 Jul 03	4750, 0.5, -0.2		4.7	7.21 ± 0.16	56	7.27 ± 0.18	8
CC Lyr	24.2	2004 Aug 9	6250, 1.0, -3.5		3.5	3.83 ± 0.04	2	3.73	1
		2005 Jul 3	6250, 1.0, -3.3		4.5	3.32 ± 0.04	2
RX Lib	24.9	2005 Apr 24	5250, 0.0, -1.0		2.9	6.50 ± 0.17	61	6.43 ± 0.15	14
TW Cap	28.6	2004 Dec 8	5250, 0.5, -1.8		3.1	5.70 ± 0.13	91	5.73 ± 0.14	31
		2005 Jul 3	6000, 0.0, -1.8		3.8	5.66 ± 0.14	33	5.64 ± 0.18	13
V1711 Sgr	28.6	2005 Jul 3	5000, 0.5, -1.2		4.1	6.28 ± 0.16	67	6.28 ± 0.17	15

^a The value of T_{eff} is in kelvins; log g is in cgs, [Fe/H] in dex.

^b The symbol ξ_t represents the microturbulence determined from the Fe I lines.

^c The column headed log ϵ gives the mean abundance relative to H (with log $\epsilon_{\text{H}} = 12.00$). The standard deviations of the means, as calculated from the line-to-line scatter, are given. The quantity n is the number of considered lines.

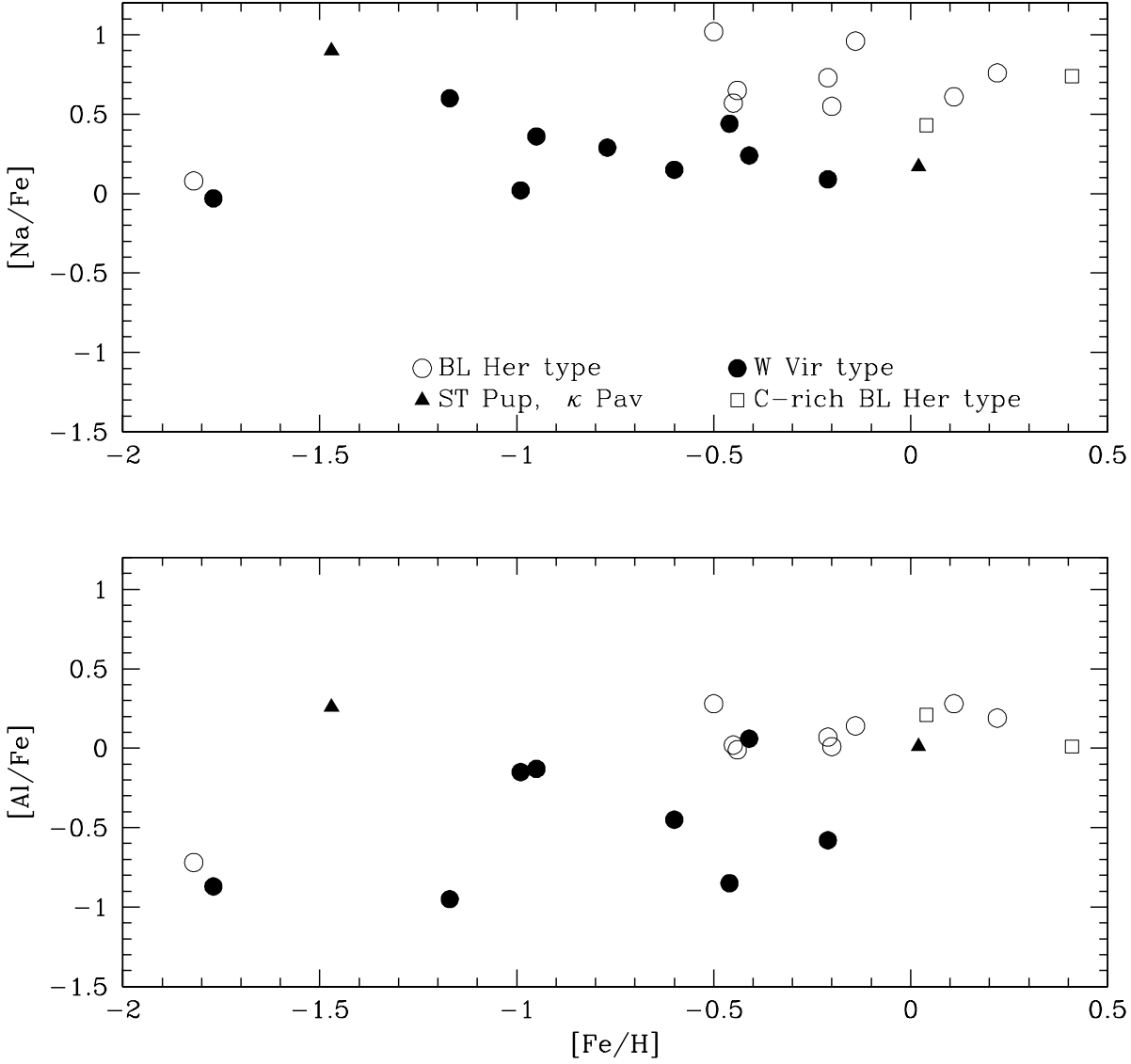


Fig. 3.— The $[Na/Fe]$ (top panel) and $[Al/Fe]$ (bottom panel) ratios versus $[Fe/H]$. The key to the symbols is given in the top panel. Symbols: unfilled circles – Our BL Her stars, filled circles – Our W Vir stars, unfilled squares – The C-rich BL Her stars RT TrA and V553 Cen, filled triangles – The W Vir stars κ Pav at $[Fe/H] \simeq 0.0$ and ST Pup at $[Fe/H] \simeq -1.5$.

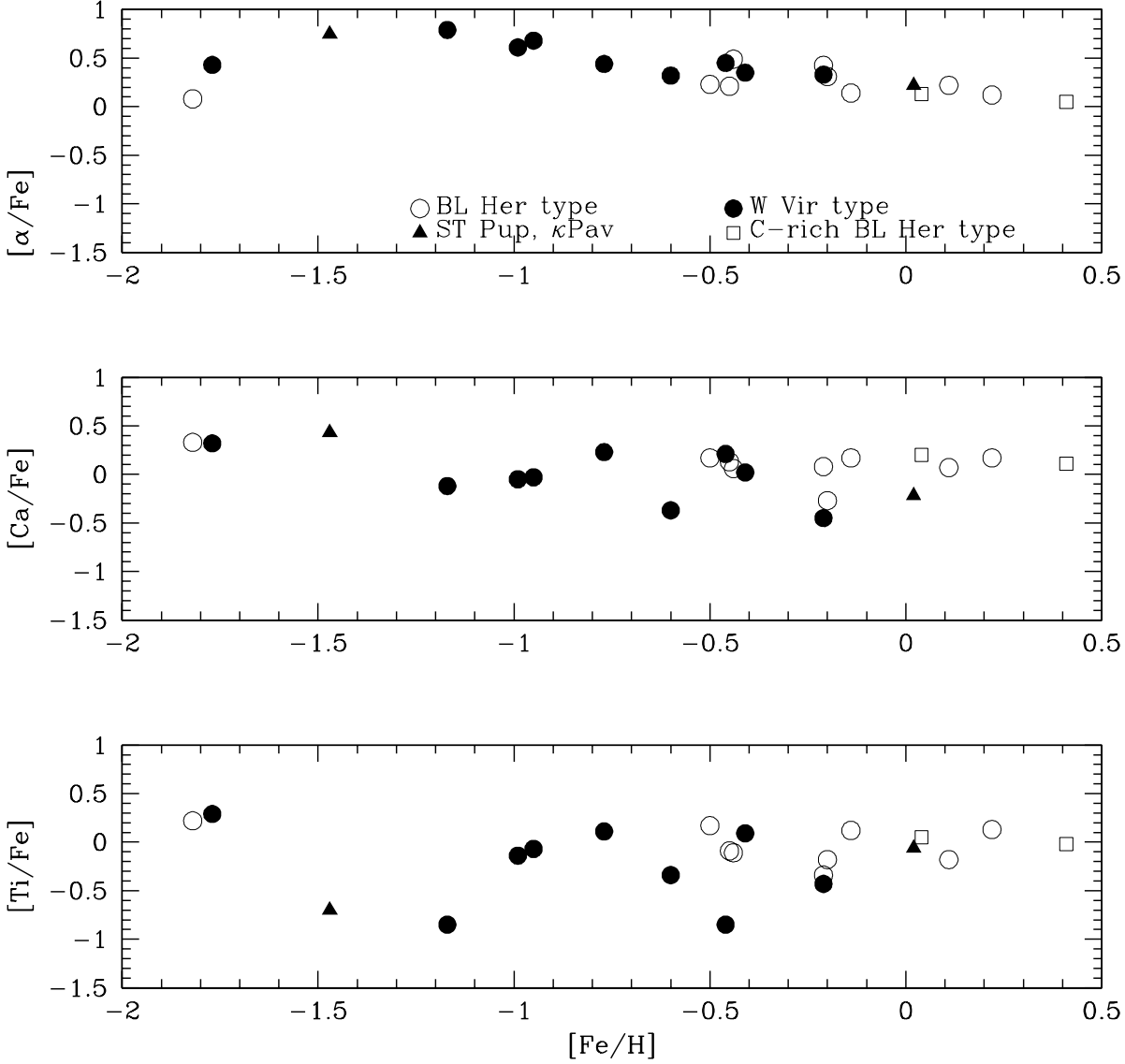


Fig. 4.— The run of the abundances of α -elements with $[\text{Fe}/\text{H}]$. The top panel shows the ratio $[\alpha/\text{Fe}]$ versus $[\text{Fe}/\text{H}]$ where $[\alpha/\text{Fe}]$ is the mean of the ratios $[\text{Mg}/\text{Fe}]$, $[\text{Si}/\text{Fe}]$, and $[\text{S}/\text{Fe}]$. The middle panel shows $[\text{Ca}/\text{Fe}]$ versus $[\text{Fe}/\text{H}]$. The bottom panel shows $[\text{Ti}/\text{Fe}]$ versus $[\text{Fe}/\text{H}]$. Symbols are as in Figure 3.

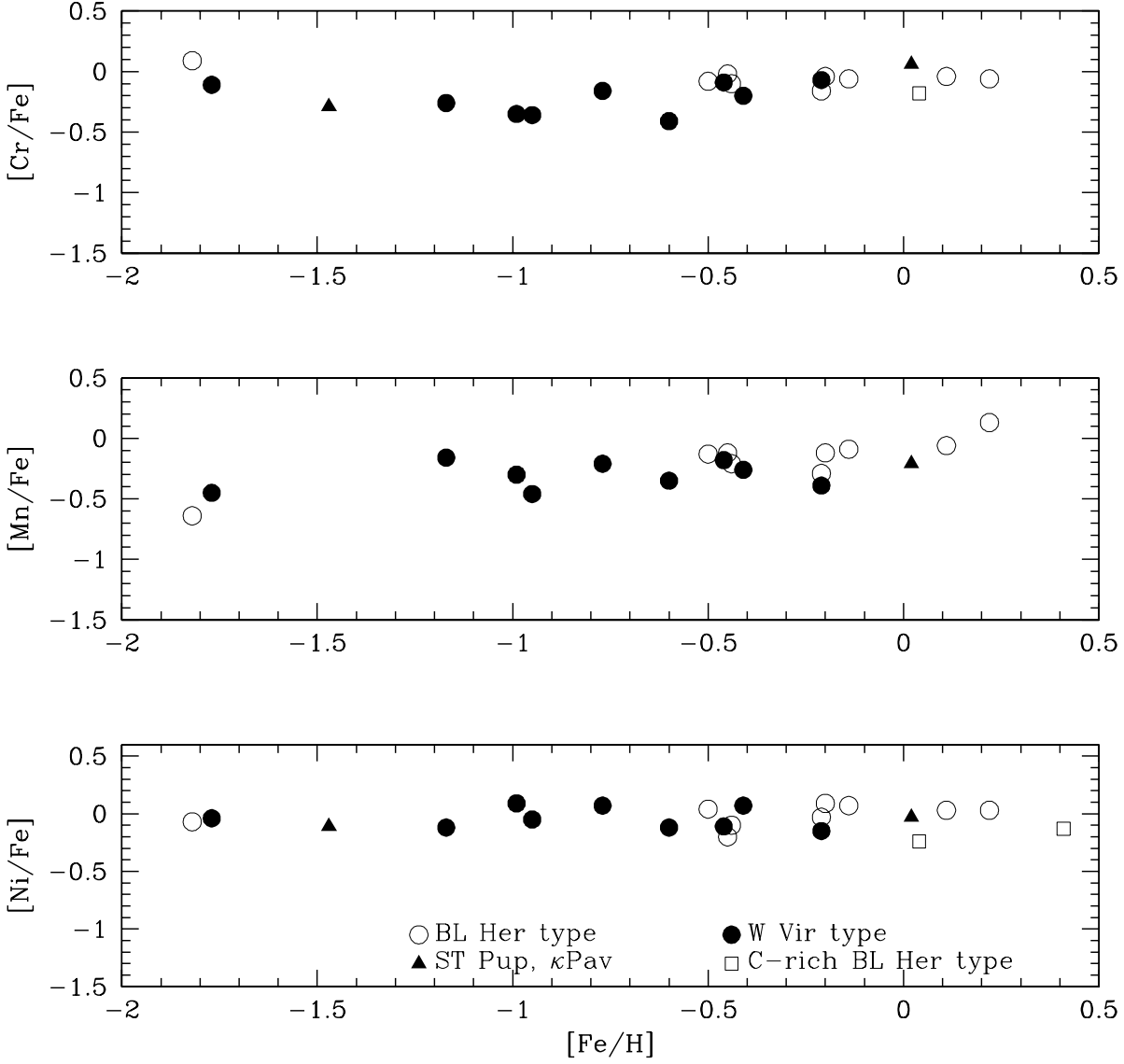


Fig. 5.— The run of the ratios $[Cr/Fe]$ (top panel), $[Mn/Fe]$ (middle panel), and $[Ni/Fe]$ (bottom panel) versus $[Fe/H]$. Symbols are as in Figure 3.

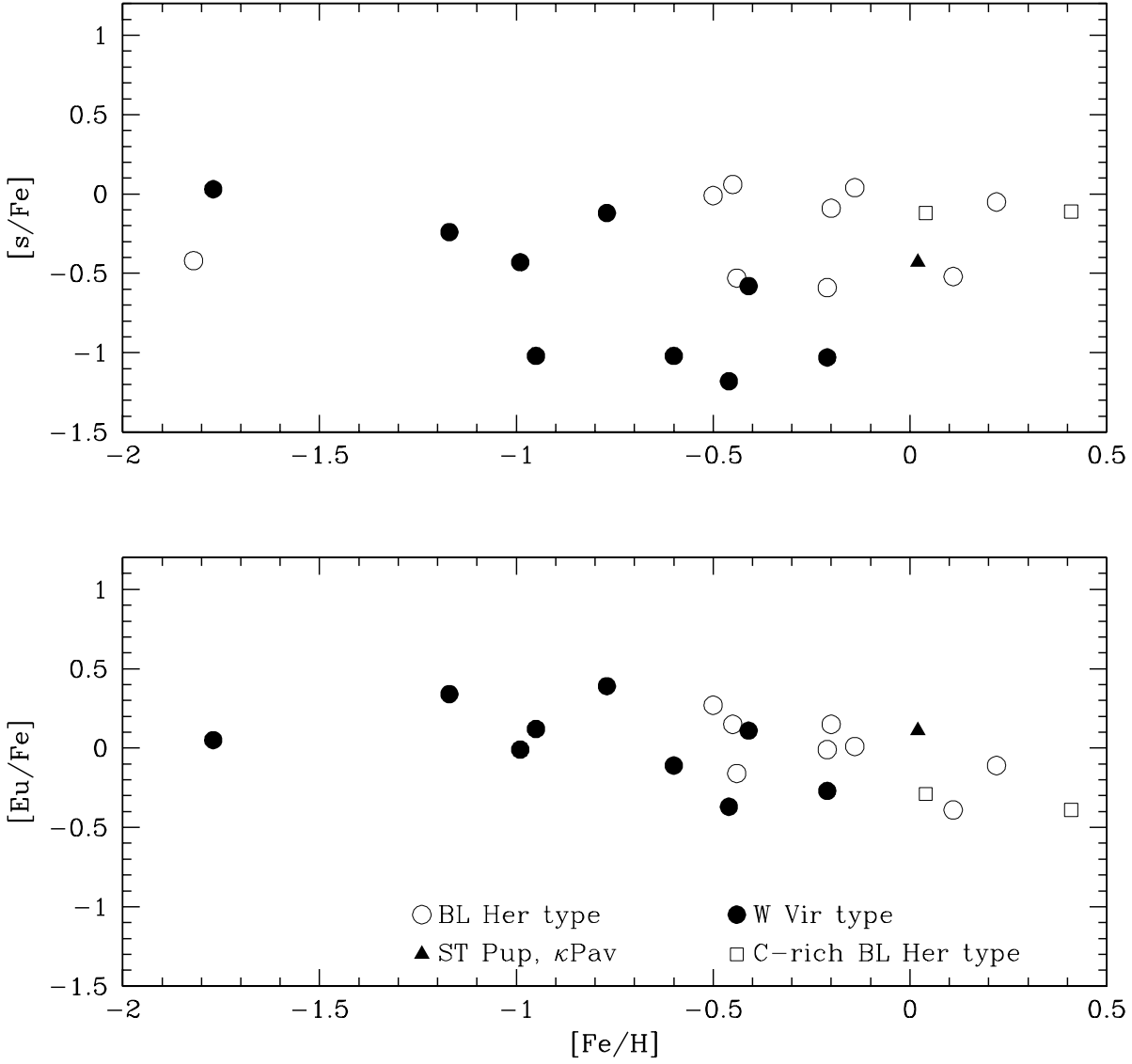


Fig. 6.— The run of the ratio $[s/Fe]$ (top panel) and $[Eu/Fe]$ (bottom panel) versus $[Fe/H]$. See text for the elements contributing to the mean $[s/Fe]$. Symbols are as in Figure 3.

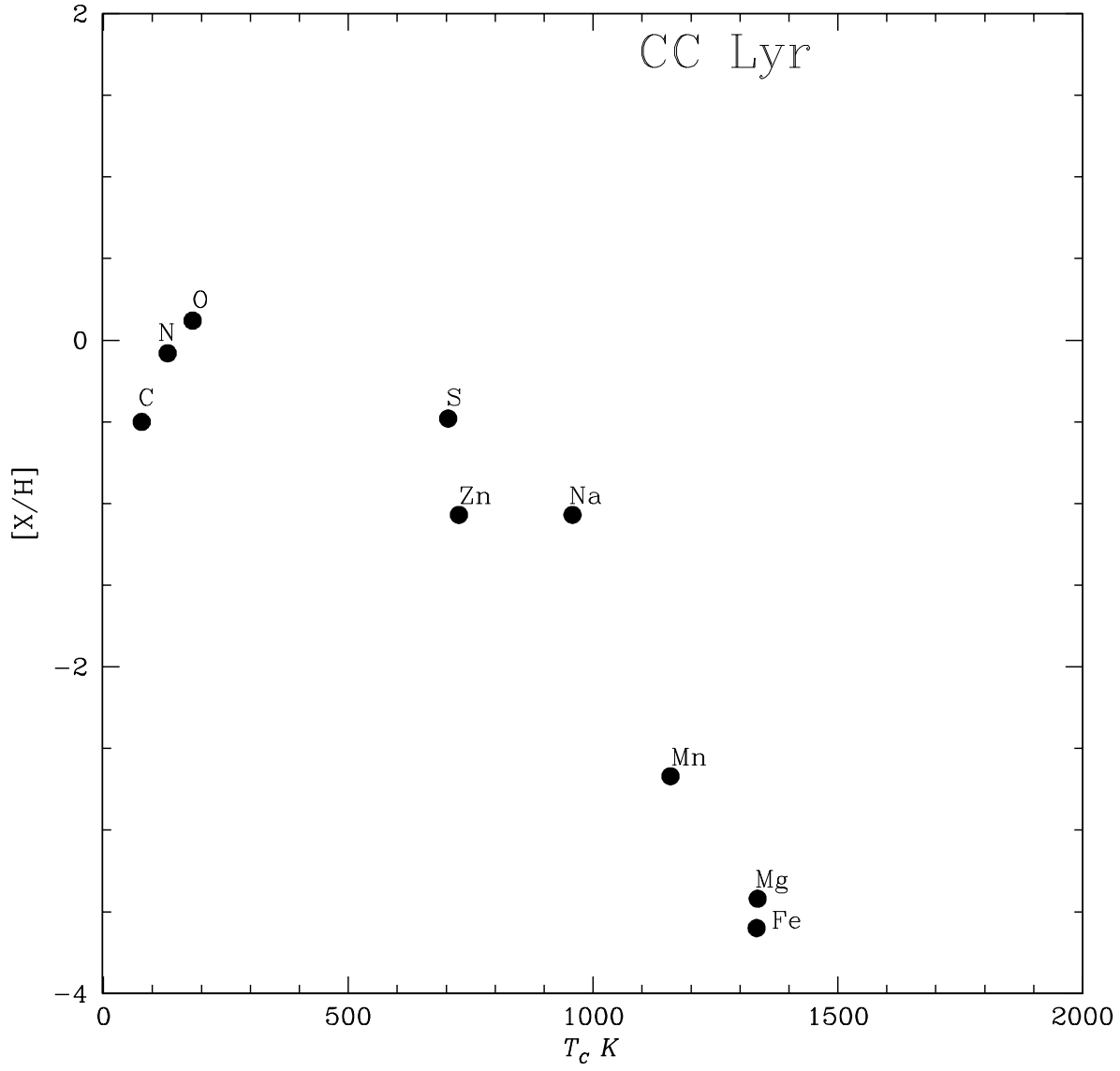


Fig. 7.— Abundances $[X/H]$ versus condensation temperature T_c for CC Lyr. Elements are identified by their chemical symbol.

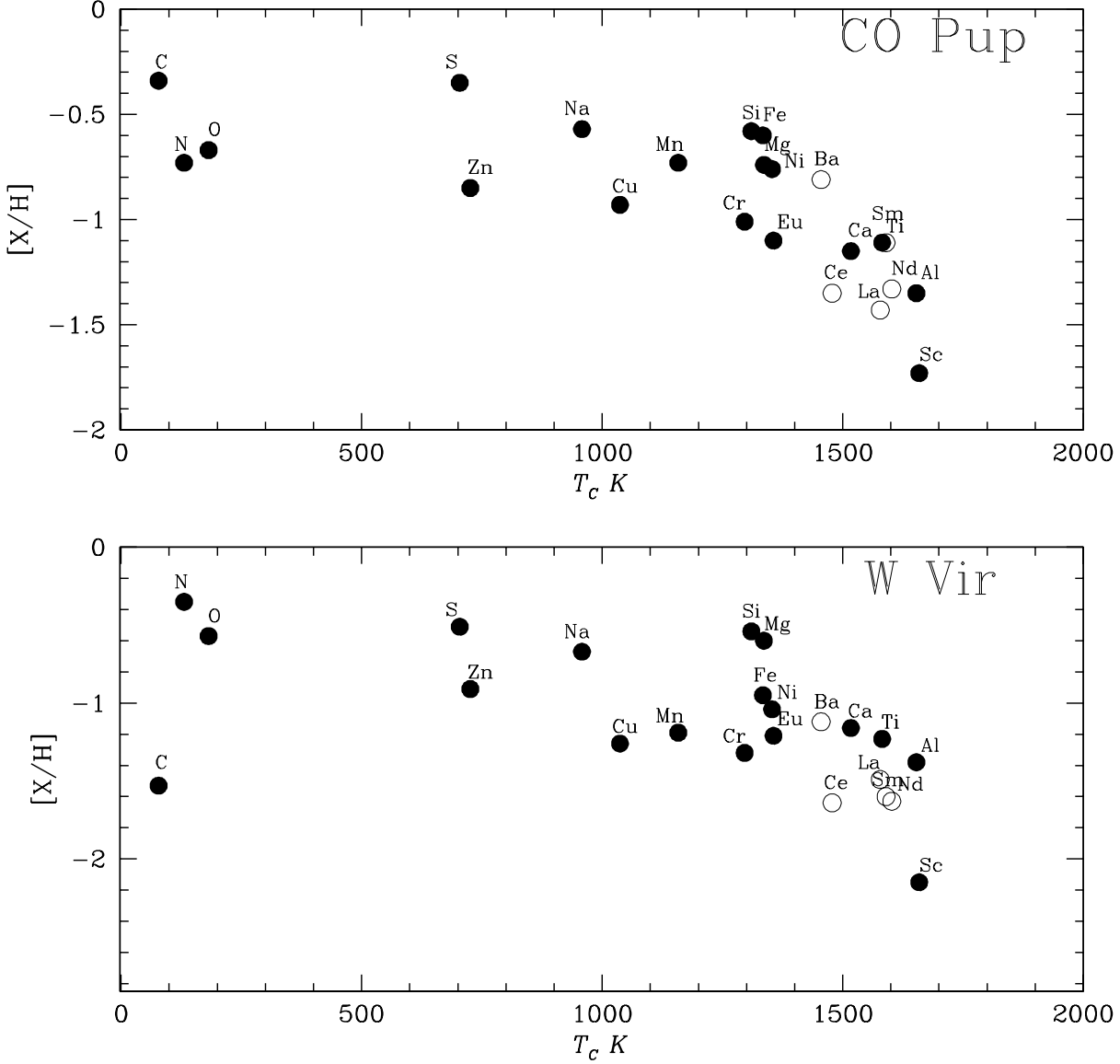


Fig. 8.— Adjusted abundances (see text) $[X/H]$ for CO Pup (top panel) and W Vir (bottom panel) versus condensation temperature T_c . Elements are identified by their chemical symbol. Unfilled circles refer to elements made principally by the s -process whose abundance might have been enhanced by thermal pulses on the AGB.

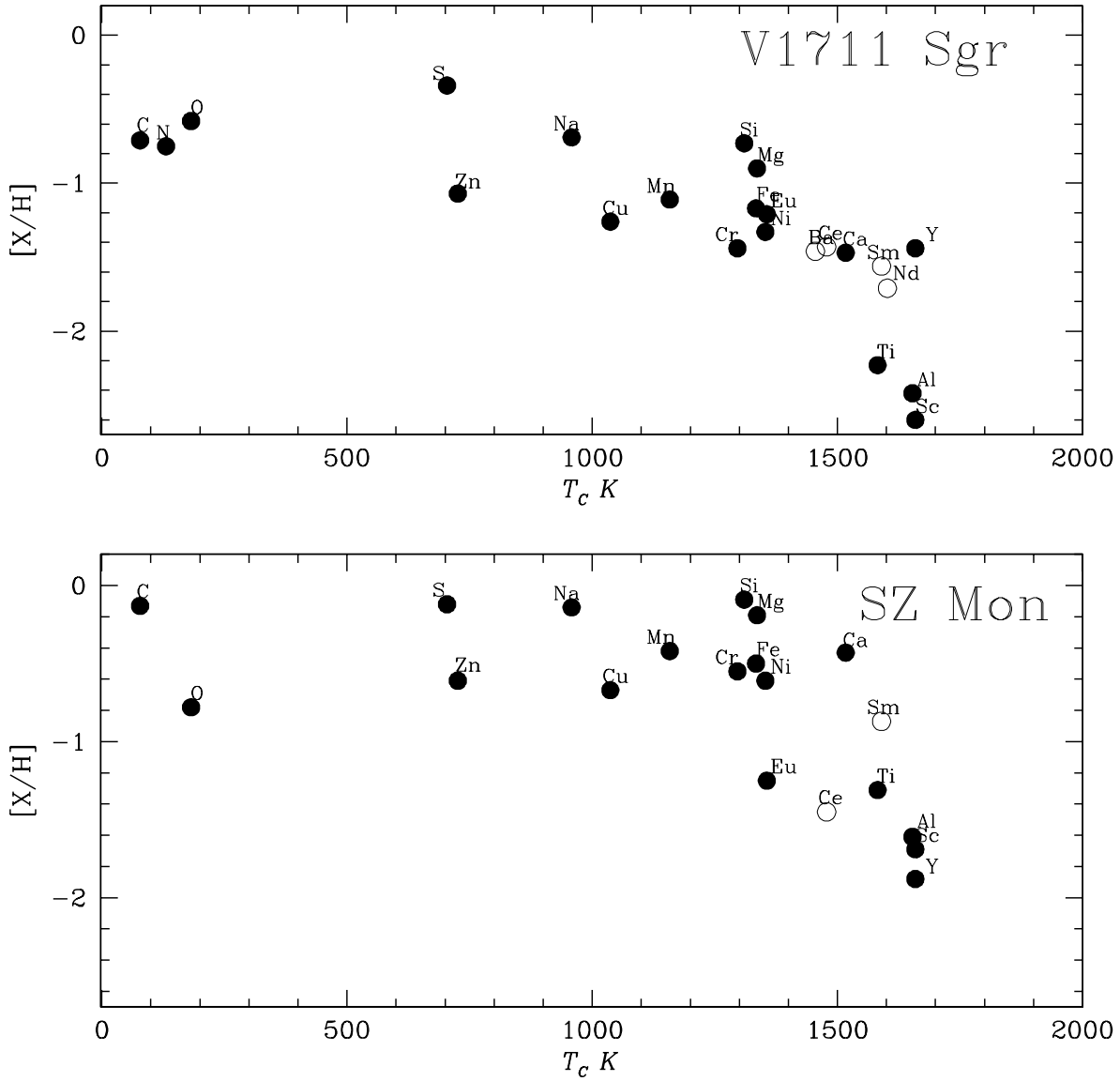


Fig. 9.— Adjusted abundances (see text) $[X/H]$ for V1711 Sgr (top panel) and SZ Mon (bottom panel) versus condensation temperature T_c . Elements are identified by their chemical symbol.

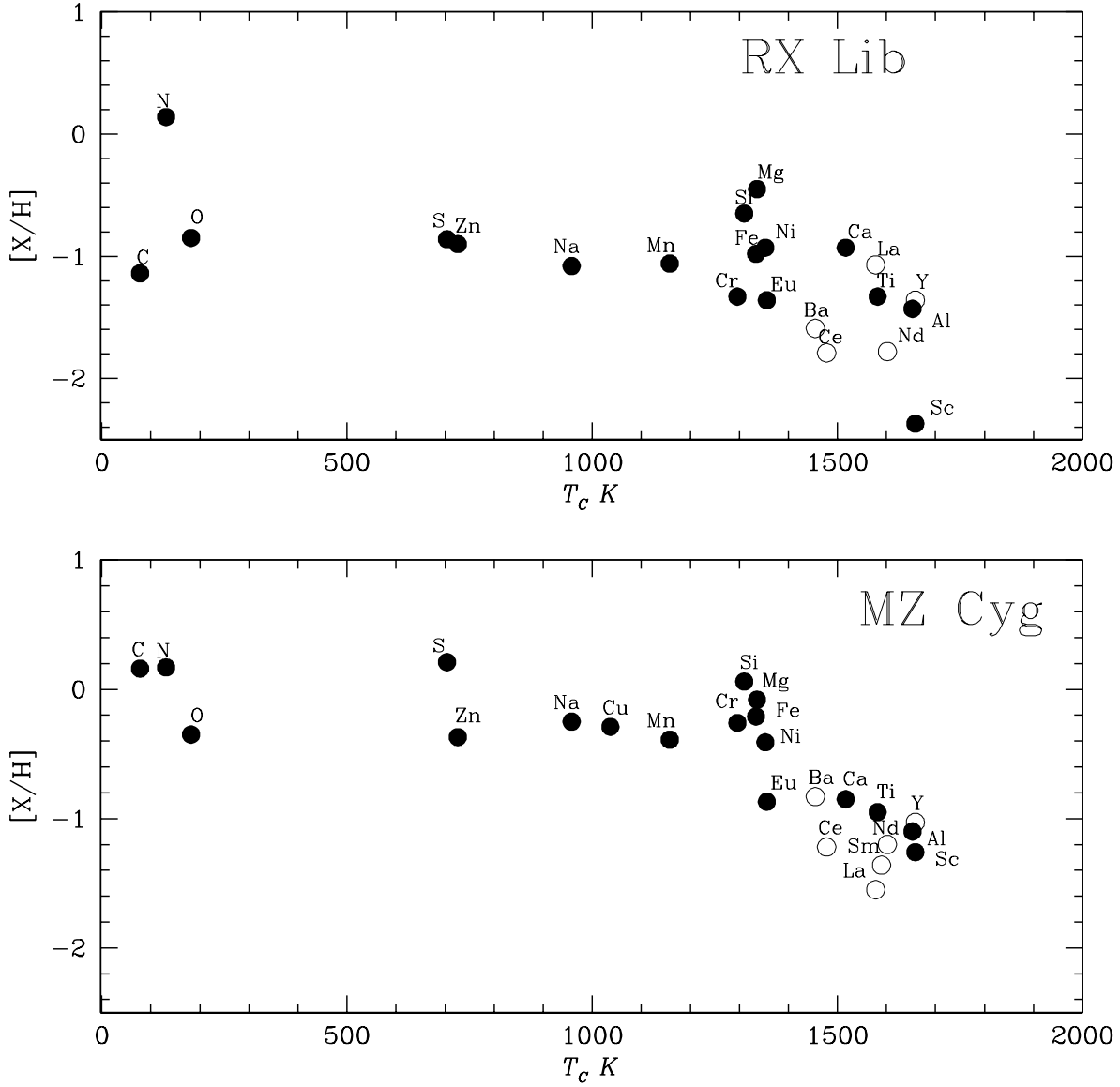


Fig. 10.— Adjusted abundances $[X/H]$ for RX Lib (top panel) and MZ Cyg (bottom panel) versus condensation temperature T_C . Elements are identified by their chemical symbol.

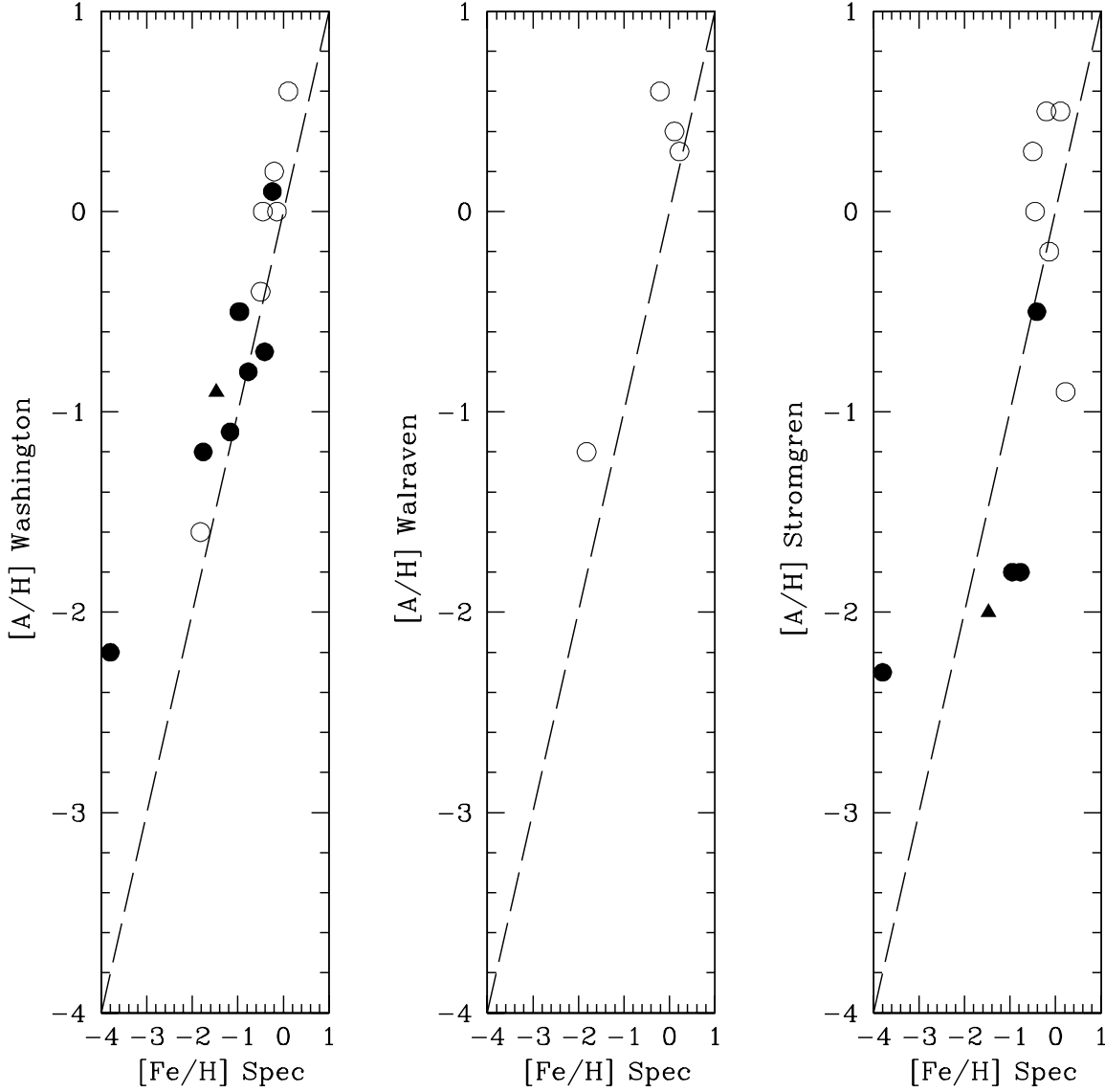


Fig. 11.— Comparisons of our spectroscopic and published photometric metallicities. The lefthand panel shows the comparison with the results from Washington photometry (Harris 1985), the middle panel with Walraven photometry (Diethelm 1990), and the righthand panel with Strömgren photometry (Meakes et al. 1991). The dashed line in each panel indicates equality between spectroscopic and photometric metallicity. The key to the symbols is given in Figure 3.

Table 2: ELEMENTAL ABUNDANCES - THE BL HER VARIABLES

Species	log ϵ_{\odot}^a	BX Del ^b		VY Pyx		BL Her		SW Tau		UY Eri		AU Peg		DQ And	
		[X/Fe]	n	[X/Fe]	n	[X/Fe]	n	[X/Fe]	n	[X/Fe]	n	[X/Fe]	n	[X/Fe]	n
C I	8.39	-0.02	14	-0.24	6	+0.44	29	+0.77	22	+0.07	5	+0.08	7
N I	7.78	+1.60	3	+1.51	3	+1.09	6	+1.26	10	<-0.1	3	+1.01	4	+0.82	4
O I	8.66	+0.41	2	+0.51	3	+0.23	5	-0.03	6	+0.52	2	+0.35	3	+0.18	3
Na I	6.17	+0.73	3	+0.65	3	+0.96	3	+0.76	3	+0.08	1	+0.55	2	+0.57	4
Mg I	7.53	+0.36	4	+0.47	4	+0.12	1	+0.02	1	+0.29	4	+0.15	3	+0.11	4
Al I	6.37	+0.07	5	-0.01	5	+0.14	3	+0.19	4	-0.72	2	+0.01	1	+0.02	4
Si I	7.51	+0.48	9	+0.33	11	+0.29	18	+0.28	17	-0.34	1	+0.29	6	+0.20	8
Si II	7.51	+0.61	2	+0.01	3	+0.06	2	+0.23	2
S I	7.14	+0.44	6	+0.54	4	+0.16	6	+0.06	6	+0.52	3	+0.32	3
Ca I	6.31	+0.08	9	+0.06	5	+0.17	19	+0.17	18	+0.33	11	-0.27	4	+0.13	7
Sc II	3.05	-0.45	4	0.00	5	+0.08	7	+0.22	8	0.00	11	+0.07	3	+0.10	6
Ti I	4.90	-0.38	2	-0.07	2	+0.14	1	+0.17	3	-0.15	4	-0.03	4
Ti II	4.90	-0.30	6	-0.16	6	+0.11	29	+0.10	17	+0.22	15	-0.21	2	-0.16	6
Cr I	5.64	-0.24	8	-0.14	6	-0.04	15	-0.05	13	+0.10	6	-0.15	3	-0.06	8
Cr II	5.64	-0.08	6	-0.06	7	-0.07	17	-0.08	18	+0.08	4	+0.06	4	+0.02	2
Mn I	5.39	-0.29	3	-0.21	5	-0.09	8	+0.13	9	-0.64	3	-0.12	2	-0.12	4
Ni I	6.23	-0.03	12	-0.10	13	+0.07	44	+0.03	45	-0.07	2	+0.09	8	-0.20	20
Cu I	4.21	+0.19	1	+0.31	1	+0.21	1	+0.38	1	-0.33	1
Zn I	4.60	-0.13	2	-0.09	3	-0.01	4	-0.03	4	-0.12	2	-0.23	2	-0.43	2
Y II	2.21	-0.66	5	-0.62	4	-0.08	7	-0.04	4	-0.42	1	+0.03	1	+0.01	5
Zr II	2.59	-0.52	2	+0.10	10	+0.03	3
Ba II	2.17	-0.29	1	-0.42	1	-0.02	3	-0.81	3	+0.70	1
La II	1.13	-0.59	1	-0.48	3	+0.10	7	+0.05	6	-0.41	2	+0.21	3
Ce II	1.58	-0.53	3	-0.52	3	-0.24	6	+0.10	5	-0.04	9
Nd II	1.45	-0.74	1	-0.60	1	+0.05	14	-0.21	1	+0.30	6
Sm II	1.01	-0.59	3	-0.21	4	-0.22	1	+0.16	2
Eu II	0.52	-0.01	2	-0.16	2	+0.01	1	-0.11	2	+0.15	1	+0.15	1
Fe I	7.45	-0.17	99	-0.40	76	-0.13	122	+0.24	115	-1.79	79	-0.19	37	-0.45	91
Fe II	7.45	-0.26	24	-0.48	12	-0.15	38	+0.21	24	-1.86	17	-0.21	11	-0.45	15

^a Solar abundances from Asplund, Grevesse, & Sauval (2005).

^b For each star, we give the mean value of [X/Fe] for element X but for Fe we give the mean [Fe/H] for the Fe I and Fe II lines. The quantity n is in all cases the number of considered lines.

Table 3: ELEMENTAL ABUNDANCES - THE INTERMEDIATE-PERIOD VARIABLES

Species	$\log \epsilon_{\odot}^a$	TX Del ^b		IX Cas		AL Vir				AP Her	
		[X/Fe]	n	[X/Fe]	n	[X/Fe] ^c	n	[X/Fe] ^d	n	[X/Fe]	n
C I	8.39	-0.04	19	-1.76	2	+0.05	11	+0.06	14	-0.09	10
N I	7.78	+1.23	6	+0.95	7	+0.88	3	+0.77	6	+0.92	6
O I	8.66	+0.36	3	+0.27	4	+0.81	2	+0.61	3	+0.69	3
Na I	6.17	+0.61	2	+1.02	3	+0.26	3	+0.22	3	+0.29	1
Mg I	7.53	+0.08	2	+0.10	1	+0.30	1	+0.36	1
Al I	6.37	+0.28	3	+0.28	4	+0.06	3
Si I	7.51	+0.32	14	+0.36	16	+0.41	17	+0.44	13	+0.53	11
Si II	7.51	+0.16	1	+0.43	2	+0.64	2
S I	7.14	+0.27	6	+0.32	5	+0.29	6	+0.36	5	+0.39	4
Ca I	6.31	+0.07	5	+0.17	13	+0.01	14	+0.03	17	+0.23	21
Sc II	3.05	-0.23	3	+0.11	8	-0.37	8	-0.32	9	-0.38	8
Ti I	4.90	+0.17	2	+0.15	4	0.11	1
Ti II	4.90	-0.18	1	+0.17	11	+0.10	8	-0.02	18	0.11	31
Cr I	5.64	0.00	4	-0.07	11	-0.17	13	-0.23	11	-0.16	10
Cr II	5.64	-0.08	3	-0.09	16	-0.20	12	-0.20	15	-0.16	16
Mn I	5.39	-0.06	4	-0.13	8	-0.26	6	-0.21	5
Ni I	6.23	+0.03	27	+0.04	35	+0.07	43	+0.06	36	+0.07	25
Cu I	4.21	+0.13	1	+0.14	1	+0.03	1
Zn I	4.60	0.00	4	+0.14	3	0.00	2	+0.06	1
Y II	2.21	-0.29	4	-0.07	11	-0.76	6	-0.56	1
Zr II	2.59	-0.55	2	+0.03	11	-0.54	2	-0.38	3	-0.25	7
Ba II	2.17	+0.13	1	-0.58	1
La II	1.13	-0.42	15	+0.17	7	-0.49	6	0.00	1
Ce II	1.58	-0.83	3	-0.16	11	-0.79	3	-0.70	1
Nd II	1.45	-0.49	9	+0.02	9	-0.49	7
Sm II	1.01	-0.19	4	-0.35	5
Eu II	0.52	-0.39	1	+0.27	2	+0.11	2	+0.39	2
Fe I	7.45	+0.11	85	-0.48	108	-0.38	85	-0.41	92	-0.75	103
Fe II	7.45	+0.11	27	-0.53	34	-0.41	27	-0.44	24	-0.80	36

^a Solar abundances from Asplund, Grevesse, & Sauval (2005).

^b For each star, we give the mean value of [X/Fe] for element X but for Fe we give the mean [Fe/H] for the Fe I and Fe II lines. The quantity n is in all cases the number of considered lines.

^c Analysis for 2004 May 3

^d Analysis for 2005 January 30

Table 4: ELEMENTAL ABUNDANCES - THE W VIR VARIABLES

Species	$\log \epsilon_{\odot}^a$	CO Pup ^b		SZ Mon		W Vir		MZ Cyg		CC Lyr			RX Lib		TW Cap			V1711 Sgr			
		[X/Fe]	n	[X/Fe]	n	[X/Fe]	n	[X/Fe]	n	[X/Fe] ^c	n	[X/Fe] ^d	n	[X/Fe]	n	[X/Fe] ^e	n	[X/Fe] ^f	n	[X/Fe]	n
C I	8.39	+0.23	3	+0.57	3	-0.23	4	+0.73	4	+3.37	4	+3.58	18	+0.19	1	<-0.1	1	+0.81	5
N I	7.78	+1.33	2	+0.39	2	+4.04	1	+1.12	2	<+0.8	2	+0.42	1
O I	8.66	+0.29	2	+0.04	2	+0.74	3	+0.18	2	+3.96	1	+3.96	3	+0.49	3	+0.70	2	<+0.5	1	+0.95	3
Na I	6.17	+0.15	4	+0.44	2	+0.36	3	+0.09	3	+2.75	1	+3.04	1	+0.02	1	+0.60	4
Mg I	7.53	+0.18	4	+0.33	3	+0.67	5	-0.02	3	+0.34	3	+0.54	3	+0.85	3	+0.45	2	+0.38	2	+0.59	4
Al I	6.37	-0.45	3	-0.85	1	-0.13	3	-0.58	3	-0.15	1	-0.87	1	-0.95	1
Si I	7.51	+0.19	5	+0.37	8	+0.55	8	+0.27	7	+0.53	5	+0.64	6	+0.52	2	+0.46	8
Si II	7.51	+0.30	2	+0.71	2	+0.57	2	+0.46	2	+0.48	2	+0.87	2
S I	7.14	+0.55	2	+0.64	2	+0.74	4	+0.73	4	+3.20	4	+3.60	5	+0.42	4	+0.40	1	+0.33	1	+1.13	4
Ca I	6.31	-0.37	6	+0.21	3	-0.03	8	-0.45	6	-0.05	5	+0.35	18	+0.29	10	-0.12	9
Sc II	3.05	-0.96	3	-1.06	2	-1.03	4	-0.87	5	-1.22	5	+0.19	6	-0.14	8	-1.26	3
Ti I	4.90	-0.39	8	-0.17	9	-0.51	3	-0.04	4	+0.38	3
Ti II	4.90	-0.28	9	-0.85	5	+0.02	6	-0.35	3	-0.24	4	+0.37	24	+0.04	5	-0.85	4
Cr I	5.64	-0.49	9	-0.04	3	-0.47	9	-0.03	2	-0.33	5	-0.18	6	+0.01	2	-0.40	9
Cr II	5.64	-0.34	5	-0.13	7	-0.26	4	-0.11	4	-0.36	4	-0.13	9	-0.15	4	-0.13	17
Mn I	5.39	-0.35	6	-0.18	4	-0.46	5	-0.39	3	+1.00	2	-0.30	2	-0.45	3	-0.16	5
Ni I	6.23	-0.12	24	-0.11	7	-0.05	24	-0.15	11	+0.09	10	+0.06	16	-0.14	2	-0.12	7
Cu I	4.21	-0.27	2	-0.15	1	-0.25	2	-0.01	1	-0.28	1	-0.03	2
Zn I	4.60	-0.13	3	-0.03	2	+0.16	4	-0.03	3	+3.05	2	+3.01	2	+0.20	4	+0.28	2	+0.01	2	+0.22	4
Y II	2.21	-1.53	1	-1.42	1	-1.92	1	-0.80	2	-0.38	1	-0.08	3	-0.11	1	-0.26	1
Zr II	2.59	-0.01	2	-0.24	1
Ba II	2.17	-0.40	1	-0.36	2	-0.90	1	-0.42	2	-0.10	2	-0.10	2
La II	1.13	-0.83	2	-0.96	3	-0.54	3	-1.32	1	-0.09	1	+0.22	4
Ce II	1.58	-0.72	5	-0.69	7	-0.97	3	-0.70	1	+0.08	4	-0.23	7
Nd II	1.45	-0.58	4	-0.53	5	-0.83	4	-0.39	1
Sm II	1.01	-0.40	2	-0.31	1	-0.55	4	-1.03	1	-0.28	1
Eu II	0.52	-0.11	2	-0.37	1	+0.12	1	-0.27	1	-0.01	2	+0.05	2	+0.34	1
Fe I	7.45	-0.64	130	-0.43	59	-0.97	110	-0.18	56	-3.62	2	-4.11	2	-0.95	61	-1.75	91	-1.79	33	-1.17	67
Fe II	7.45	-0.57	12	-0.50	8	-0.93	22	-0.24	9	-3.72	1	-1.02	14	-1.72	31	-1.81	13	-1.17	15

^a Solar abundances from Asplund, Grevesse, & Sauval (2005).

^b For each star, we give the mean value of [X/Fe] for element X but for Fe we give the mean [Fe/H] for the Fe I and Fe II lines. The quantity n is in all cases the number of considered lines. ^c Analysis for 2004 August 9

^d Analysis for 2005 March 7

^e Analysis for 2004 December 8

^f Analysis for 2005 July 3

This figure "f2.jpeg" is available in "jpeg" format from:

<http://arxiv.org/ps/0706.2029v1>